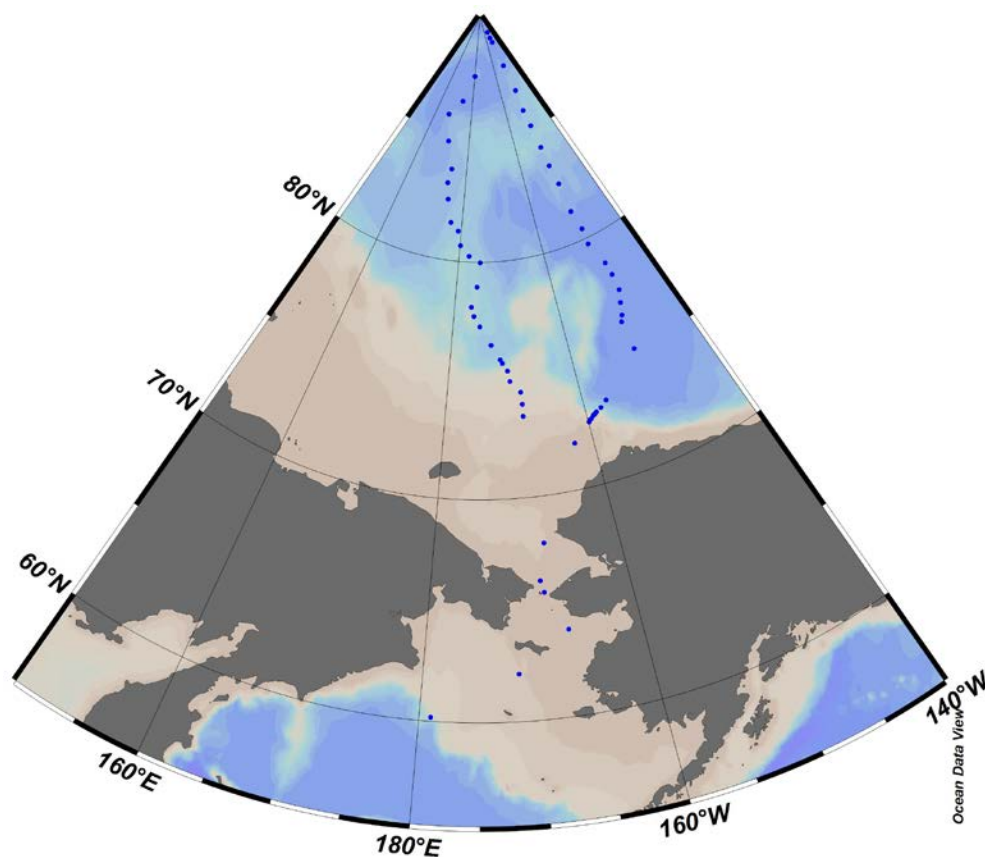


Global Ocean Repeat Hydrography Study: pH, Total Alkalinity, and Total CO₂ Measurements in the Arctic Ocean ARC01 Aug. – Oct. 2015



Frank J. Millero, Ryan J. Woosley, Andrew R. Margolin, and Fen Huang
University of Miami, Rosenstiel School of Marine and Atmospheric Science
4600 Rickenbacker Causeway
Miami, FL 33149

Please cite as: Millero, F.J., R.J. Woosley, A.R. Margolin, and F. Huang. 2016. Global Ocean Repeat Hydrography Study: pH, Total Alkalinity, and Total CO₂ Measurements in the Arctic Ocean During the R/V Healy Cruise ARC01 (9 August - 12 October, 2015): Technical Report. http://cdiac.ornl.gov/ftp/oceans/CLIVAR/ARC01_33HQ20150809/ARC01_2015_UM_Carb_Tech_Report.pdf. Carbon Dioxide Information Analysis Center, Oak Ridge National Laboratory, US Department of Energy, Oak Ridge, Tennessee. doi: 10.3334/CDIAC/OTG.CLIVAR_ARC01_33HQ20150809_TECH_REPORT

Table of Contents

List of Tables	3
List of Figures	4
1. Introduction.....	6
2. Description of Variables and Methods.....	7
2.1 Total Alkalinity.....	7
2.1.1 Sampling.....	8
2.1.2 Analyzer Description.....	8
2.1.3 Reagents	9
2.1.4 Standardization.....	10
2.2 Total Inorganic Carbon Dioxide (TCO ₂) Analysis	11
2.2.1 Sampling.....	11
2.2.2 Analyzer Description.....	11
2.2.3 Standardization.....	12
2.3 Discrete pH Analysis	12
2.3.1 Sampling.....	13
2.3.2 Analyzer Description.....	13
2.3.3 Standardization.....	15
3. Accuracy and Precision of Measurements	16
3.1 Total Alkalinity Accuracy and Precision	16
3.2 Coulometric TCO ₂ Accuracy and Precision:	27
3.3 Discrete pH Accuracy and Precision	29
4. Internal Consistency.....	31
5. Distribution of the Carbon Parameters in Seawater Along the ARC01 Track	34
6. Decadal Changes in Carbon Parameters (1994-2015)	38
6.1 Changes in Surface Measurements	39
6.2 Changes Between the AOS 2005 and the GO-SHIP ARC01 2015	46
6.3 Changes Between the AOS94 and the GO-SHIP ARC01	53
References.....	58
Appendices.....	60
A. Waypoint Coordinates and Bottom Depth of the ARC01 2015 Cruise	60
B. Diagram of an Automated Total Alkalinity System	62
C. Diagram of an Automated pH System.....	63
D. Data Format Description	63

List of Tables

Table 1. The assigned values of CRM batch 146 provided by A. Dickson, SIO.....	10
Table 2. Comparison of the measured TA ($\mu\text{mol}\cdot\text{kg}^{-1}$), TCO ₂ ($\mu\text{mol}\cdot\text{kg}^{-1}$), and pH with the values of the CRM from Cells A and B.....	17
Table 3. Comparison of measurements of TA, TCO ₂ , and pH of the same sample on the two systems.....	21
Table 4. Accuracy and precision of spectrophotometric pH measurements using CRM, TRIS buffer, and duplicate measurements.....	29
Table 5. Difference between the measured and calculated values of TA, TCO ₂ , and pH.	32

List of Figures

Figure 1. The difference between the measured TA ($\mu\text{mol}\cdot\text{kg}^{-1}$) with the certified value of 2214.11 $\mu\text{mol}\cdot\text{kg}^{-1}$ (Batch 146) on a.) Cell A and b.) Cell B. Solid lines are the means and dashed lines are 2 times the standard deviations.....	18
Figure 2. The difference between the measured $\text{TCO}_{2\text{pot}}$ ($\mu\text{mol}\cdot\text{kg}^{-1}$) with the certified value of 2002.92 (Batch 146) for a.) Cell A and b.) Cell B. Solid lines are the means, dashed lines are 2 times the standard deviations.	19
Figure 3. Difference between the measured pH_{pot} and calculated value of 7.9045 (CRM Batch 146) for a.) Cell A and b.) Cell B. The solid lines are the means, and dashed lines are 2 times the standard deviations.....	20
Figure 4. Precision of TA ($\mu\text{mol}\cdot\text{kg}^{-1}$), $\text{TCO}_{2\text{pot}}$ ($\mu\text{mol}\cdot\text{kg}^{-1}$) and pH_{pot} measurements between Cells A and B. The dashed lines are 2 standard deviations from the means (solid lines).....	23
Figure 5. The reproducibility of TA ($\mu\text{mol}\cdot\text{kg}^{-1}$), $\text{TCO}_{2\text{pot}}$ ($\mu\text{mol}\cdot\text{kg}^{-1}$), and pH_{pot} on Cell A. The dashed lines are 2 standard deviations from the means (solid lines).	24
Figure 6. The reproducibility of TA ($\mu\text{mol}\cdot\text{kg}^{-1}$), $\text{TCO}_{2\text{pot}}$ ($\mu\text{mol}\cdot\text{kg}^{-1}$), and pH_{pot} on Cell B. The dashed lines are 2 standard deviations from the means (solid lines).	25
Figure 7. Difference between the TCO_2 ($\mu\text{mol}\cdot\text{kg}^{-1}$) measured by SOMMA and potentiometry (top), and the difference between pH measured by spectrophotometry and potentiometry (bottom). The dashed lines are 2 standard deviations from the means (solid lines).	26
Figure 8. Difference between measured TCO_2 ($\mu\text{mol}\cdot\text{kg}^{-1}$) and certified value of CRM. Dashed lines are 2 standard deviations from the mean (solid line).	27
Figure 9. Duplicate measurements of TCO_2 ($\mu\text{mol}\cdot\text{kg}^{-1}$) measured on the SOMMA instrument. Dashed lines are 2 standard deviations from the mean (solid line).	28
Figure 10. Precision of spectrophotometric pH measurements using duplicates (1 st measurement - 2 nd measurement). The dashed lines are 2 times the standard deviation from the mean (solid line).....	30
Figure 11. Difference between the pH measured by spectrophotometry and potentiometry. The dashed lines are 2 standard deviations from the mean (solid line).	31
Figure 12. Difference between the measured and calculated values of TA, TCO_2 , and pH. The input variables for the calculated values are shown in parentheses. The dashed lines are 2 standard deviations from the means (solid lines).	33
Figure 13. Measured TA in $\mu\text{mol}\cdot\text{kg}^{-1}$. Left panels show the Makarov Basin section from south to north (left to right), and right panels show the Canada Basin section from north to south (left to right).....	35
Figure 14. Measured TCO_2 in $\mu\text{mol}\cdot\text{kg}^{-1}$. Left panels show the Makarov Basin section from south to north (left to right), and right panels show the Canada Basin section from north to south (left to right).	36
Figure 15. Measured pH at 25°C. Left panels show the Makarov Basin section from south to north (left to right), and right panels show the Canada Basin section from north to south (left to right).	37
Figure 16. Comparison of the surface (<40 db) salinity between the AOS94 and ARC01 cruises in the upper panel, and AOS05 and ARC01 cruises in the lower panel.	40

Figure 17. Comparison of the surface (<40 db) oxygen between the AOS94 and ARC01 cruises in the upper panel, and AOS05 and ARC01 cruises in the lower panel.	41
Figure 18. Comparison of the surface (<40 db) TA between the AOS94 and the ARC01 cruises in the upper panel, and the AOS05 and ARC01 cruises in the lower panel.	42
Figure 19. Comparison of the surface (<40 db) NTA between the AOS94 and ARC01 cruises in the top panel, and the AOS05 and ARC01 cruises in the bottom panel.	43
Figure 20. Comparison of the surface (<40 db) TCO ₂ between the AOS94 and the ARC01 cruises in the upper panel, and the AOS05 and ARC01 cruises in the lower panel.	44
Figure 21. Comparison of the surface (<40 db) NTCO ₂ between the AOS94 and ARC01 cruises in the top panel, and the AOS05 and ARC01 cruises in the bottom panel.	45
Figure 22. Comparison of the surface (<40 db) pH at 25°C between the AOS-2005 and ARC01 cruises. The AOS05 data were measured at 15°C and were corrected to 25°C using TA and CO ₂ sys.	46
Figure 23. Changes in TA between the 2005 and 2015 occupations of the Canada Basin section.	48
Figure 24. Changes in NTA between the 2005 and 2015 occupations of the Canada Basin.	49
Figure 25. Changes in TCO ₂ between the 2005 and 2015 occupations of the Canada Basin.	50
Figure 26. Changes in NTCO ₂ between the 2005 and 2015 occupations of the Canada Basin section.	51
Figure 27. Changes in pH between the 2005 and 2015 occupations of the Canada Basin section.	52
Figure 28. Changes in TA between 1994 and 2015 occupations of Makarov Basin section.	54
Figure 29. Changes in NTA between 1994 and 2015 in the Makarov Basin section.	55
Figure 30. Changes in TCO ₂ between 1994 and 2015 occupations of the Makarov Basin section.	56
Figure 31. Changes in NTCO ₂ between the 1994 and 2015 occupations of the Makarov Basin section.	57

1. Introduction

The ARC01 cruise consisted of a loop through the Arctic Ocean's Canadian Basin, which comprises of two sections in the Canada and Makarov Basins, sampled from 9 August – 13 October 2015. The U.S. Coast Guard Cutter *Healy* departed Dutch Harbor Alaska on 9 August, traversed the Makarov Basin, reaching the North Pole on 5 September, and returning via the Canada Basin arriving back in Dutch Harbor on 13 October. This cruise was part of a decadal series of repeat hydrography sections jointly funded by the NOAA [Climate Program Office](#) and the [National Science Foundation Division of Ocean Sciences](#) as part of the Climate Variability and Predictability Study (CLIVAR) CO₂ Repeat Hydrography Program, which was updated in 2007 to the Global Ocean Ship-based Hydrographic Investigations Program ([GO-SHIP](#)). The repeat hydrography program focuses on the need to monitor inventories of CO₂, heat and freshwater and their transports in the ocean. Earlier programs under WOCE, JGOFS, and CLIVAR have provided baseline observational fields for these parameters. The new measurements will reveal much about the changing patterns on decadal scales. The program serves as a structure for assessing changes in the ocean's biogeochemical cycle in response to natural and/or human-induced activity. The cruise was combined with the GEOTRACES program measuring a wide variety of trace metals, allowing both programs to complete their goals and complement each other on the same cruise.

The Makarov Basin transect was a repeat of the 1994 AOS94 cruise, and the Canada Basin transect was a repeat of the 2005 AOS05 cruise. The full cruise track is shown in the figure on the cover. Underway measurements of surface seawater (partial pressure of CO₂ (pCO₂), temperature, and salinity) and atmospheric measurements (CFCs

and aerosols) were also made along the cruise track. The complete coordinates of the waypoints can be found in Appendix A.

Fifty-one scientists from twenty academic institutions participated in the cruise. Our group measured total alkalinity (TA) by potentiometry, total inorganic carbon dioxide (TCO₂) by coulometry and potentiometry, and pH by spectrophotometry and potentiometry. The final dataset for all measured parameters for the GO-SHIP portion is freely available at the Carbon Dioxide Information Analysis Center (CDIAC) (<http://cdiac.ornl.gov/oceans/RepeatSections/>). Only the TA, coulometric TCO₂, and spectrophotometric pH are reported to CDIAC. Trace metal data is reported to the GEOTRACES data office.

2. Description of Variables and Methods

TA, TCO₂, and pH are the main variables determined by our group. The use of a closed cell titration allows us to also determine the TCO₂ and pH by potentiometry, providing a check on our systems; these values are not reported to CDIAC since this method provides lower precision than other methods used on the cruise. A detailed description of the methods is found below.

2.1 Total Alkalinity

Total alkalinity can be conceptually thought of as the sum of the excess bases in seawater or the buffering capacity. The principle components are carbonate and bicarbonate, with small contributions from borate and other bases. The standard method for determination is through potentiometric titration with hydrochloric acid (HCl). Details of the sampling collection and analysis are given below.

2.1.1 Sampling

Samples for TA were drawn from the 10 L Niskin-type bottles into 500 cm³ borosilicate bottles using silicone tubing that fit over the petcock. This tubing helped both to avoid contaminating dissolved organic carbon (DOC) samples and allowed samples to be filled from the bottom, entraining little to no bubbles. Bottles were rinsed with a small volume of water and then filled from the bottom, overflowing at least half of the volume. Approximately 15 cm³ of water was withdrawn from the flask by arresting the sample flow and removing the sampling tube, thus creating a small expansion volume and a reproducible headspace. The sample bottles were sealed at a ground glass joint with a glass stopper. The samples were thermostated at 25°C before analysis. At repeat hydrography stations, duplicate samples were taken near the surface, the bottom, and the oxygen minimum layer. Due to water budget constraints, duplicates could not be collected at GEOTRACES stations.

2.1.2 Analyzer Description

The total alkalinity of seawater was evaluated from the proton balance at the alkalinity equivalence point, $\text{pH}_{\text{equiv}} = 4.5$ at 25°C. The method utilizes a multi-point HCl titration of seawater according to the definition of TA (Dickson, 1981). The potentiometric titrations of seawater using a closed cell give values of TA and TCO₂. The pH is also determined from the initial EMF (electromotive force) measurement before the addition of acid. To distinguish between values of TCO₂ and pH made by the different methods, the subscript pot is used for potentiometric measurements; when no subscript is used it refers to the coulometric or spectrophotometric method for values of TCO₂ and pH respectively, unless otherwise noted.

Two titration systems, A and B, were used for measuring TA. Each system used a Metrohm 665 or 765 Dosimat titrator, an Orion 720A pH meter and a custom designed plexiglass water-jacketed closed titration cell (Millero *et al.*, 1993b). The seawater samples were equilibrated to a constant temperature of $25 \pm 0.1^\circ\text{C}$ with a water bath (ThermoFisher Haak A10). The water-jacketed cell has a volume of $\sim 200\text{ cm}^3$. Each cell has a fill and drain valve that is electronically activated to increase the reproducibility of the volume of sample. A typical titration recorded the EMF after the readings became stable (deviation less than 0.09 mV) and then enough acid was added to change the voltage a pre-assigned increment (13 mV). A full titration (~ 25 points) takes about 20 minutes. The electrodes used to measure the EMF of the sample consisted of a ROSS glass pH electrode (Orion, model 810100) and a double junction Ag, AgCl reference electrode (Orion, model 900200).

An integrated program controls the titration, data collection, and the calculation of the carbonate parameters (TA, pH_{pot} , and $\text{TCO}_{2\text{pot}}$; Millero *et al.*, 1993b). The program is patterned after those developed by Dickson (1981), Johansson and Wedborg (1982), and Dickson *et al.* (2007). The program uses a Levenberg-Marquardt nonlinear least-squares algorithm to calculate E^0 , pH_{pot} , TA, $\text{TCO}_{2\text{pot}}$ and pK^*_1 from the potentiometric titration data. A diagram of the system is shown in Appendix B.

2.1.3 Reagents

A single 50 L batch of $\sim 0.25\text{ m}$ HCl acid was prepared in 0.45 m NaCl by dilution of concentrated HCl (AR Select, Mallinckrodt), to yield a total ionic strength similar to seawater of salinity 35.0 ($I = 0.7\text{ M}$). The acid was standardized with alkalinity titrations on certified reference material (CRM). The calibrated normality of the acid used was

0.24361 \pm 0.0001 N HCl. The acid was stored in 500-mL glass bottles sealed with Apiezon[®] M grease for use at sea.

Table 1. The assigned values of CRM batch 146 provided by A. Dickson, SIO.

Batch 146	
<i>Parameter</i>	<i>Assigned Value</i>
Salinity	33.122
Total Alkalinity	2214.11 \pm 0.68 $\mu\text{mol kg}^{-1}$
Total Dissolved Inorganic Carbon	2002.92 \pm 0.67 $\mu\text{mol kg}^{-1}$
pH _{sws} * (at 25°C)	7.9045
Phosphate	0.34 $\mu\text{mol kg}^{-1}$
Silicate	1.8 $\mu\text{mol kg}^{-1}$
Nitrite	0.01 $\mu\text{mol kg}^{-1}$
Nitrate	0.22 $\mu\text{mol kg}^{-1}$
*Calculated from TCO ₂ and TA using the dissociation constants of Millero <i>et al.</i> (2006) and boron concentration of Lee <i>et al.</i> (2010)	

2.1.4 Standardization

The volumes of the cells used were calibrated to \pm 0.03 cm³ while in port, in Dutch Harbor, before the start of the cruise by multiple titrations using CRMs provided by Dr. Andrew Dickson, Marine Physical Laboratory, La Jolla, California. The certified values for the batch used are given in table 1. Calibrations of the burette of the Dosimat with water at 25°C indicate that the systems deliver 3.000 cm³ (the approximate value for a titration of seawater) to a precision of \pm 0.0004 cm³, resulting in an error of \pm 0.3 $\mu\text{mol}\cdot\text{kg}^{-1}$ in TA. The reproducibility and precision of measurements are checked using low nutrient surface seawater collected from the ship's flowing seawater system and CRMs. CRMs were utilized in order to account for instrument drift and to maintain measurement precision. Duplicate analyses provide additional quality assurance and were

taken from the same Niskin bottle. Duplicates were either measured both on the same instrument (A or B) or one measured on each system (A and B). Reported TA values were corrected using the average ratio of the certified CRM value to measured value on each system.

2.2 Total Inorganic Carbon Dioxide (TCO₂) Analysis

TCO₂ is simply the sum of all CO₂ species dissolved in seawater:

$$\text{TCO}_2 = [\text{CO}_2^*] + [\text{HCO}_3^-] + [\text{CO}_3^{2-}] \quad (1)$$

It is determined analytically by the addition of acid to convert all species to gaseous CO₂, then measured coulometrically.

2.2.1 Sampling

The TCO₂ water samples were drawn from 10 L Niskin-type bottles into cleaned, pre-combusted 500 cm³ borosilicate glass bottles using silicon tubing. Bottles were rinsed with a small volume and filled from the bottom, overflowing by at least one-half volume. Care was taken not to entrain any bubbles. The tube was pinched off and withdrawn, creating a ~15 mL headspace, then 0.400 mL of saturated HgCl₂ solution was added as a preservative. The sample bottles were sealed with glass stoppers lightly covered with Apiezon®-L grease, and were thermostated to 20°C in a water bath for a minimum of 20 minutes prior to analysis.

2.2.2 Analyzer Description

The DIC analytical equipment (DICE) was designed based upon the original SOMMA systems (Johnson *et al.*, 1985, 1987, 1993; Johnson, 1992). These new systems have improved on the original design by use of more modern National Instruments

electronics and other available technology. In the coulometric analysis of TCO_2 , all carbonate species are converted to CO_2 (gas) by addition of excess hydrogen to the seawater sample using 8.5% H_3PO_4 . The evolved CO_2 gas is carried into the titration cell of the coulometer, where it reacts quantitatively with a proprietary reagent based on ethanolamine to generate hydrogen ions. These are subsequently titrated with coulometrically generated OH^- . CO_2 is thus measured by integrating the total charge required to achieve this (Dickson *et al.*, 2007).

2.2.3 Standardization

The coulometer was calibrated by injecting aliquots of pure CO_2 (99.995%) by means of an 8-port valve outfitted with two calibrated sample loops of different sizes (~1 mL and ~2 mL; Wilke *et al.*, 1993). The instrument was calibrated at the beginning of each cell with a minimum of two sets of the gas loop injections. A total of 211 loop calibrations were run during this cruise.

Secondary standards were run throughout the cruise. These standards are CRM provided by Dr. Andrew Dickson, Marine Physical Laboratory, La Jolla, California. Their accuracy is determined manometrically on land in San Diego. TCO_2 data reported here have been corrected to the CRM batch 146 value (table 1) using the ratio of the certified to measured values.

2.3 Discrete pH Analysis

The pH is measured using an indicator dye and a spectrophotometer. In seawater there are several different definitions or scales for pH, which complicates the measurement. The three main scales used are the free scale (pH_F), which only includes the concentration of the free proton ($[\text{H}^+]_\text{F}$), the total scale (pH_T) defined as:

$$\text{pH}_T = [\text{H}^+]_F + [\text{HSO}_4^-] \quad (2)$$

and the seawater scale defined as:

$$\text{pH}_{\text{sws}} = [\text{H}^+]_F + [\text{HSO}_4^-] + [\text{HF}] \quad (3)$$

The subscripts F, T, and SWS are used to distinguish between the free, total, and seawater scales, respectively. All values reported here are on the seawater scale unless otherwise noted.

2.3.1 Sampling

At each station samples were drawn directly from the Niskin-type bottles on the rosette into 50 cm³ borosilicate glass syringes using polycarbonate Luer-lock 3-way valves that fit directly on the petcock of the Niskin bottle. The syringes were rinsed completely with the sample and then filled while taking care not to entrain any bubbles. After collection the syringe was checked for bubbles and any found were ejected. The samples were thermostated at 20 or 25°C in a water bath before analysis.

2.3.2 Analyzer Description

Measurements of the pH_T of seawater were first made using the multi-wavelength spectrophotometric techniques of Clayton and Byrne (1993), which were calibrated using TRIS buffers (Ramette *et al.*, 1977, Millero *et al.*, 1993a). The values were then converted to pH_{sws} using the dissociation constants of H_2SO_4 (Dickson, 1990) and HF (Dickson and Riley, 1979). The Sulphonphthalein indicator m-cresol purple (mCp) was used to make the pH measurements following the methods of Clayton and Byrne (1993) as modified by Lee *et al.* (1996), using the equations of Liu *et al.* (2011). Purified indicator (batch 7) was provided by Dr. Robert Byrne (University of South Florida). The system is patterned after the standard operating procedure developed by the U.S.

Department of Energy (DOE) (Dickson *et al.*, 2007). The automated system performs discrete analysis of pH on samples approximately every 6 minutes using a total of 40 cm³ of sample. The syringes are stored in a water bath at 25°C or 20°C to maintain a constant temperature. A refrigerated circulating temperature bath (Neslab, model RTE-10) regulates the temperature of the sample at 25 or 20 ± 0.05°C. A microprocessor controlled syringe pump (Kloehn V6) with a 10 cm³ syringe and sampling valve aspirates and injects the seawater sample into the 10 cm micro-volume optical cell (Starna Cells, Inc.) at a precisely controlled rate. The syringe pump rinses and primes the optical cell with 20 cm³ of sample and the software permits 90 seconds for temperature stabilization. An Agilent 8453 UV/VIS spectrophotometer measures background absorbance of the sample. The automated syringe pump and sampling valves aspirates 9.98 cm³ seawater and 0.02 cm³ of indicator and injects the mixture into the cell. After the software permits 90 seconds for temperature stabilization, a Hart 1523 digital platinum resistance thermometer measures the temperature and the spectrophotometer acquires the absorbance at 434, 578, 730, and 488 nm. The full spectra from 190-900 nm at 1 nm intervals are also archived. A diagram of the system is shown in Appendix C.

The addition of indicator slightly perturbs the pH of the sample. To account for this an indicator correction must be made. This is done by making additional measurements on a subset of the samples (approximately 1 per station), in which the sample is measured a second time using twice the amount of indicator. It was insured that the entire pH range was adequately covered over the course of the cruise. The change in the absorbance ratio (ΔR) was then determined by fitting the measurements to the following equation:

$$\Delta R = A + BR \quad (4)$$

where A is the y-intercept, B is the slope, and R is the absorbance ratio from a single addition of indicator. The corrected absorbance ratio (R_{corr}) is then calculated using:

$$R_{\text{corr}} = R + (A + BR) * (A_{488} - A_{730}) \quad (5)$$

The absorbance at the isosbestic point (488 nm) is used instead of the volume of the indicator as was done by Clayton and Byrne (1993) because it is more precise than assuming a constant volume of indicator is added. The values of A and B used for this cruise were 0.0379 and -0.0551, respectively.

2.3.3 Standardization

There are currently no certified standards for which to standardize measurements of pH. The current practice is to use pH measurements made on batches of TRIS buffer, and CRMs. The expected pH of the CRM is calculated from the certified values of TA and TCO_2 and is given in table 1.

An 8 L batch of TRIS buffer was prepared in the lab before the cruise according to the recipe of Millero *et al.* (1993a). This does not include any fluoride so values are reported on the total scale. The TRIS was stored in 500 cm³ borosilicate bottles sealed with ground glass stoppers and Apiezon[®] M grease. Part way through the cruise something began growing in the TRIS bottles, which is common and illustrates one of the issues in developing a certified pH standard. The growth does not appear to affect the pH of the buffer, as shown by the TRIS measurements discussed in section 3.3.

About halfway through the cruise the water bath used to control the temperature of the pH system would no longer heat to 25°C. Starting at station 32 all samples were measured at 20°C and corrected to exactly 25°C. For CRMs and samples with TA

measurements the temperature correction was done using CO2sys and the equations of Millero *et al.* (2006). For samples without TA (N = 29) the temperature was corrected according to the equation (Millero, 2007):

$$\text{pH}_{25} = \text{pH}_{\text{meas}} - 0.01528 * (25 - t_{\text{meas}}) \quad (6)$$

where t_{meas} is the measured temperature in degrees Celsius and pH_{meas} is the measured pH at t_{meas} . TRIS buffer has a different temperature dependence than that of seawater. In order to correct the TRIS measurements to 25°C a slope of 0.03164 (determined from equation 6 of Liu *et al.*, 2011) was used in equation 6.

3. Accuracy and Precision of Measurements

The accuracy and precision of all measurements were checked using several different methods. For TA and TCO₂, CRMs were used to determine accuracy. For pH, there is no certified standard, but CRMs were also measured and compared to the values calculated from the certified TA and TCO₂. The precision of TA was checked using low nutrient surface seawater collected in 20 L batches as needed from the ship's flowing seawater system. A TRIS buffer was used to check the precision and accuracy of the pH samples. For all parameters, duplicates were also measured on each repeat hydrography station to check precision. Due to water budget constraints, duplicates could not be measured on GEOTRACES stations. Details of the results are given in the following sections. CRM batch 146 was used for this cruise; the certified TA and TCO₂ values, along with the calculated pH_{sws} , are shown in table 1.

3.1 Total Alkalinity Accuracy and Precision

A total of 1,266 unique samples were collected and analyzed for TA. Of those, 7.1% were duplicates and 2.4% were flagged as questionable or bad. Several methods

were used to determine the accuracy and precision of the TA measurements. A comparison of measured potentiometric values of TA, TCO_{2pot}, and pH_{pot} made on CRMs during the cruise are given in table 2 and shown in figure 1 (TA), figure 2 (TCO_{2pot}), and figure 3 (pH_{pot}). Values of TCO₂ and pH from bottles obtained after analysis on spectrophotometric and coulometric systems are not reported due to probable loss of CO₂ after opening.

The precision in the measured values of TA, TCO₂ and pH are reasonable and consistent with other studies. The average measured value for TA is in good agreement with the assigned value. The measured values of TCO₂ are higher than the assigned value as found in previous studies (Millero *et al.*, 1993b). The station data for TA and TCO_{2pot} have been corrected to the CRM values using the ratio of the certified value to measured value. The average correction for TA was 1.30 $\mu\text{mol}\cdot\text{kg}^{-1}$, with a maximum correction of 2.75 $\mu\text{mol}\cdot\text{kg}^{-1}$.

Table 2. Comparison of the measured TA ($\mu\text{mol}\cdot\text{kg}^{-1}$), TCO₂ ($\mu\text{mol}\cdot\text{kg}^{-1}$), and pH with the values of the CRM from Cells A and B.

Cell A				
Parameter	Mean	stdev	N	Meas-CRM
TA	2211.51	2.43	30	-2.60
TCO _{2pot}	2010.42	3.11	17	7.32
pH _{pot}	7.887	0.005	17	-0.017
Cell B				
TA	2213.46	2.28	39	-0.65
TCO _{2pot}	2012.41	2.76	9	9.49
pH _{pot}	7.887	0.006	9	-0.017

TA CRM Measurements

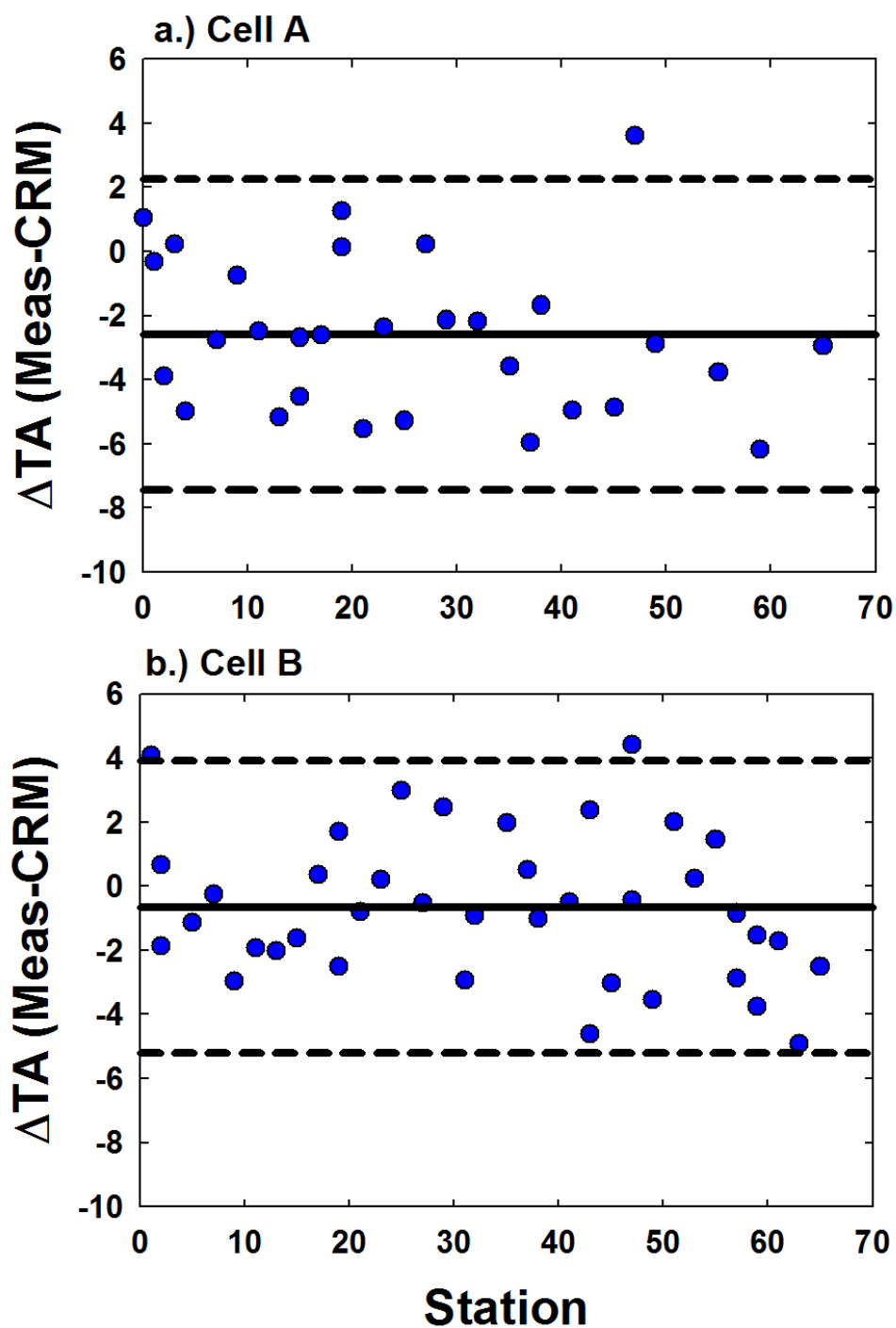


Figure 1. The difference between the measured TA ($\mu\text{mol}\cdot\text{kg}^{-1}$) with the certified value of $2214.11 \mu\text{mol}\cdot\text{kg}^{-1}$ (Batch 146) on a.) Cell A and b.) Cell B. Solid lines are the means and dashed lines are 2 times the standard deviations.

TCO_{2pot} CRM Measurements

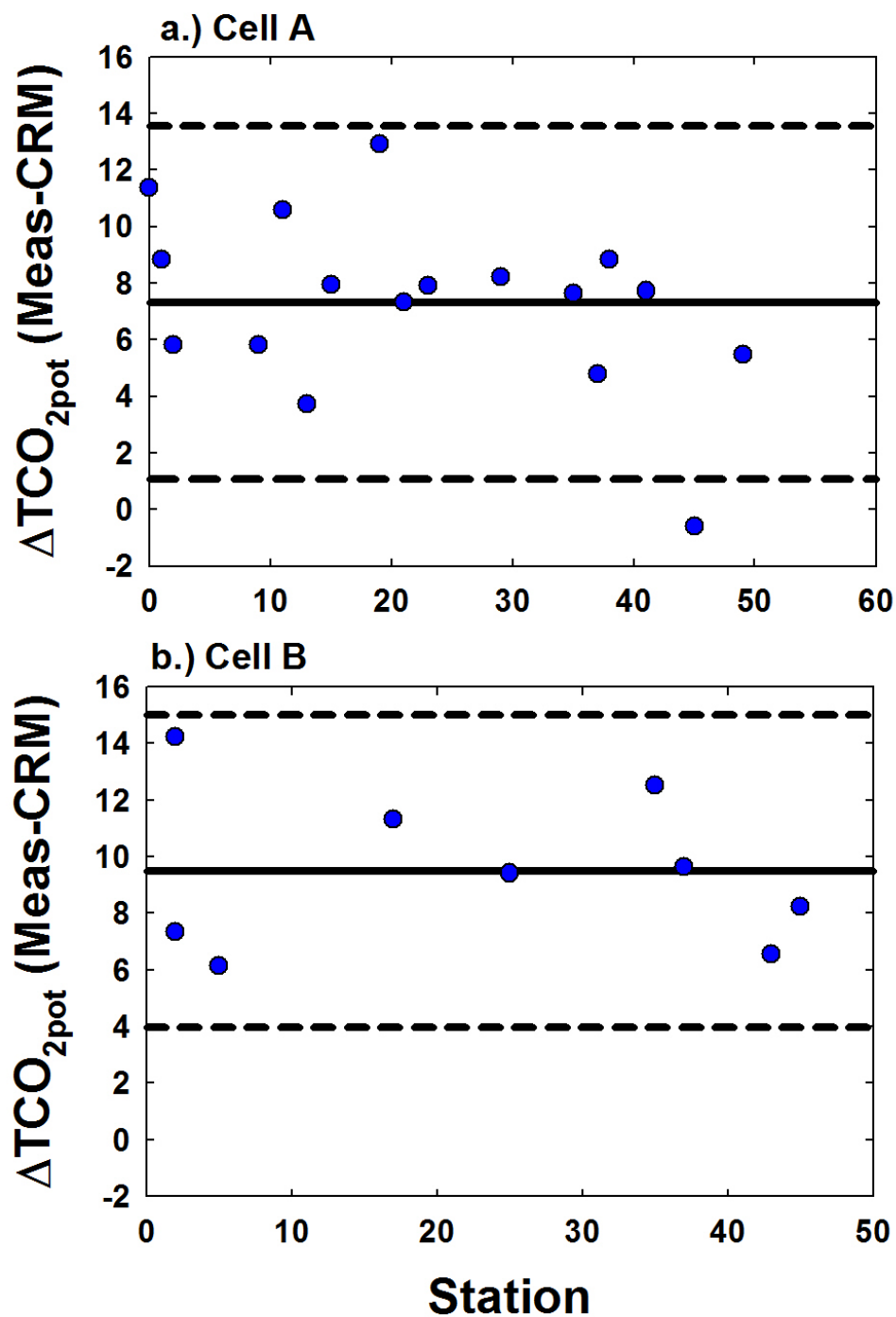


Figure 2. The difference between the measured TCO_{2pot} ($\mu\text{mol}\cdot\text{kg}^{-1}$) with the certified value of 2002.92 (Batch 146) for a.) Cell A and b.) Cell B. Solid lines are the means, dashed lines are 2 times the standard deviations.

pH_{pot} CRM Measurements

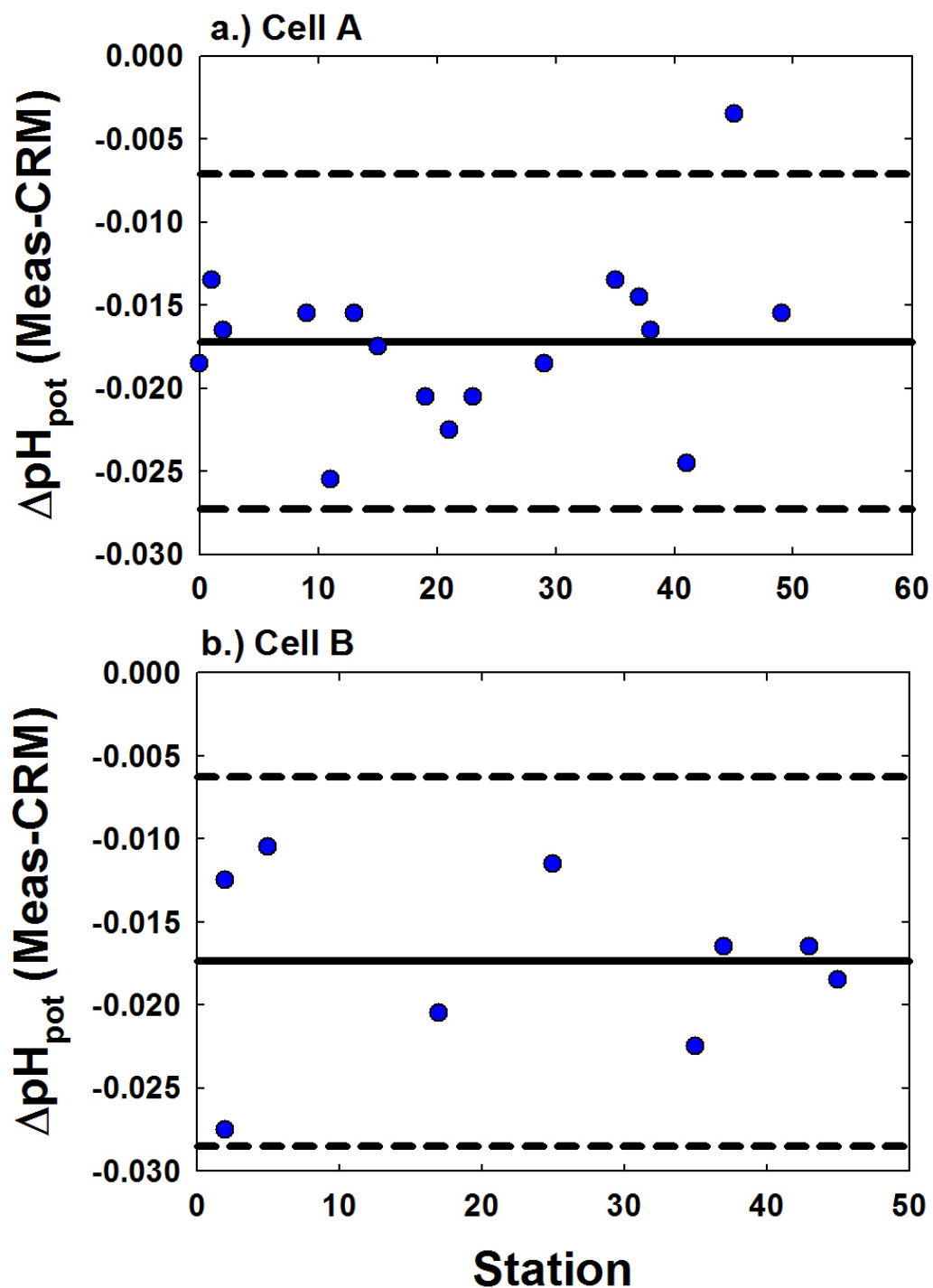


Figure 3. Difference between the measured pH_{pot} and calculated value of 7.9045 (CRM Batch 146) for a.) Cell A and b.) Cell B. The solid lines are the means, and dashed lines are 2 times the standard deviations.

Although the potentiometric values of pH are relatively precise, they were offset on both systems by 0.017. This has been found in earlier studies and is probably related to the non-Nernstian behavior of the electrodes. Thus, an adjustment was made to all station pH_{pot} values using the offset between measured values and the calculated CRM value.

A total of 8 batches of low nutrient surface seawater collected from the ship's flowing seawater system were used on the cruise. The precision (standard deviation) averaged less than $2.5 \mu\text{mol}\cdot\text{kg}^{-1}$, with the largest standard deviation being $3.8 \mu\text{mol}\cdot\text{kg}^{-1}$.

The reproducibility of the measurements was also checked by comparing the results of both systems on seawater sampled from the same Niskin bottle. The results for the duplicate measurements are given in table 3 and shown in figures 4-6. The standard deviations in both TA and $\text{TCO}_{2\text{pot}}$ on the same systems are close to $2 \mu\text{mol}\cdot\text{kg}^{-1}$, and slightly higher between the systems. The standard deviations of the pH_{pot} is about 0.005. These are typical precisions for at sea measurements using this method.

Table 3. Comparison of measurements of TA, TCO_2 , and pH of the same sample on the two systems.

	System	A - B	A	B
TA ($\mu\text{mol}\cdot\text{kg}^{-1}$)	Mean	-0.13	0.40	-0.46
	Stdev	3.70	1.80	2.13
	N	22	33	36
$\text{TCO}_{2\text{pot}}$ ($\mu\text{mol}\cdot\text{kg}^{-1}$)	Mean	-0.60	0.70	-0.10
	Stdev	3.82	2.28	2.56
	N	21	33	37
pH_{pot}	Mean	0.0032	0.0004	0.0001
	Stdev	0.0052	0.0049	0.0040
	N	23	34	37

The TCO_2 was also measured using the more precise SOMMA method, which uses coulometry. The difference between the $\text{TCO}_{2\text{SOMMA}}$ and $\text{TCO}_{2\text{pot}}$ is shown in figure 7. The mean difference is $4.5 \pm 4.8 \mu\text{mol}\cdot\text{kg}^{-1}$ ($N = 941$). These values are reasonable, although it would seem the correction of $\text{TCO}_{2\text{pot}}$ to the CRM is a slight over correction. The pH measured by spectrophotometry was also compared to the pH measured by potentiometry. The differences are shown in figure 7. The mean and standard deviation is -0.003 ± 0.007 ($N = 1226$). These values are reasonable and comparable to previous studies.

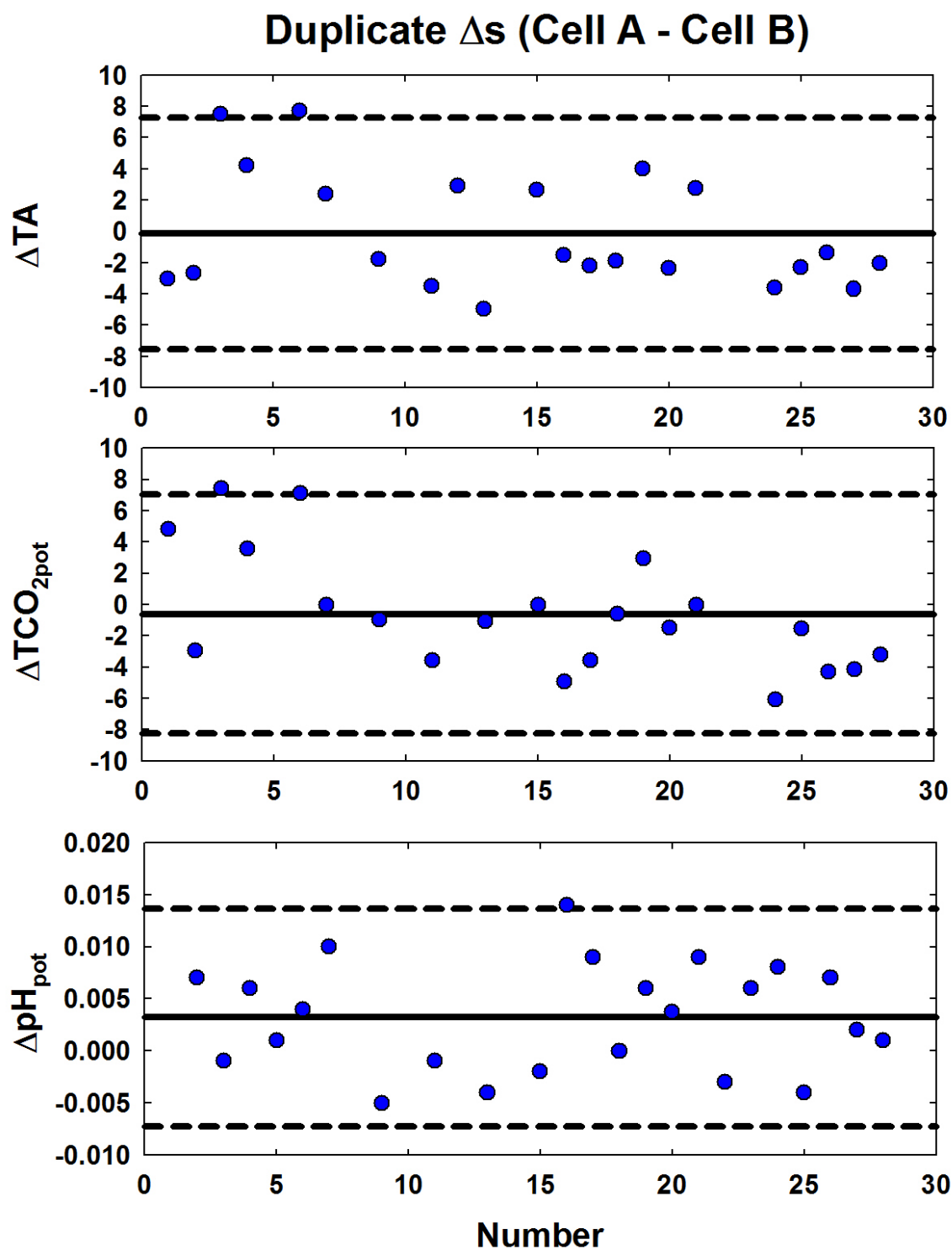


Figure 4. Precision of TA ($\mu\text{mol}\cdot\text{kg}^{-1}$), $\text{TCO}_{2\text{pot}}$ ($\mu\text{mol}\cdot\text{kg}^{-1}$) and pH_{pot} measurements between Cells A and B. The dashed lines are 2 standard deviations from the means (solid lines).

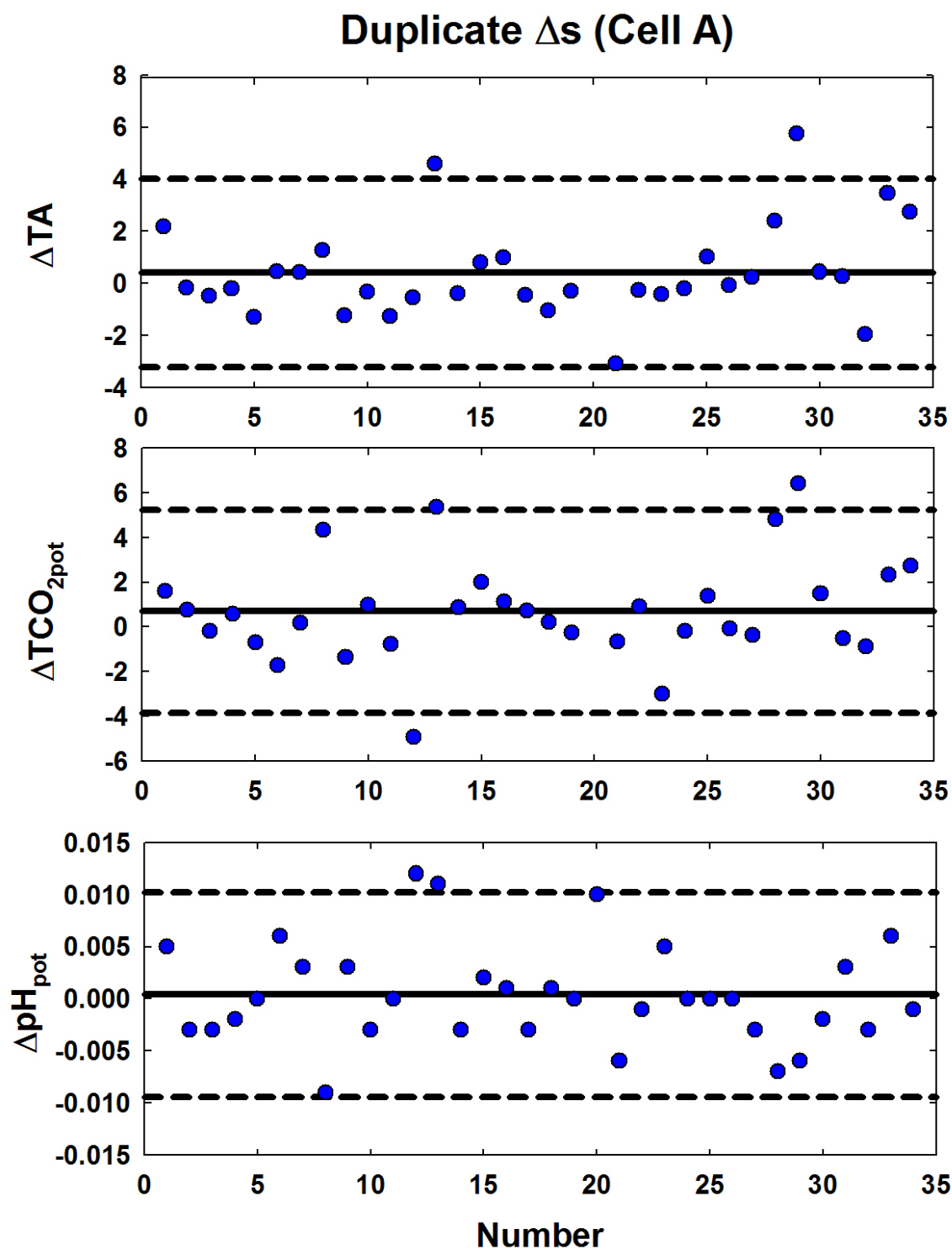


Figure 5. The reproducibility of TA ($\mu\text{mol}\cdot\text{kg}^{-1}$), $\text{TCO}_{2\text{pot}}$ ($\mu\text{mol}\cdot\text{kg}^{-1}$), and pH_{pot} on Cell A. The dashed lines are 2 standard deviations from the means (solid lines).

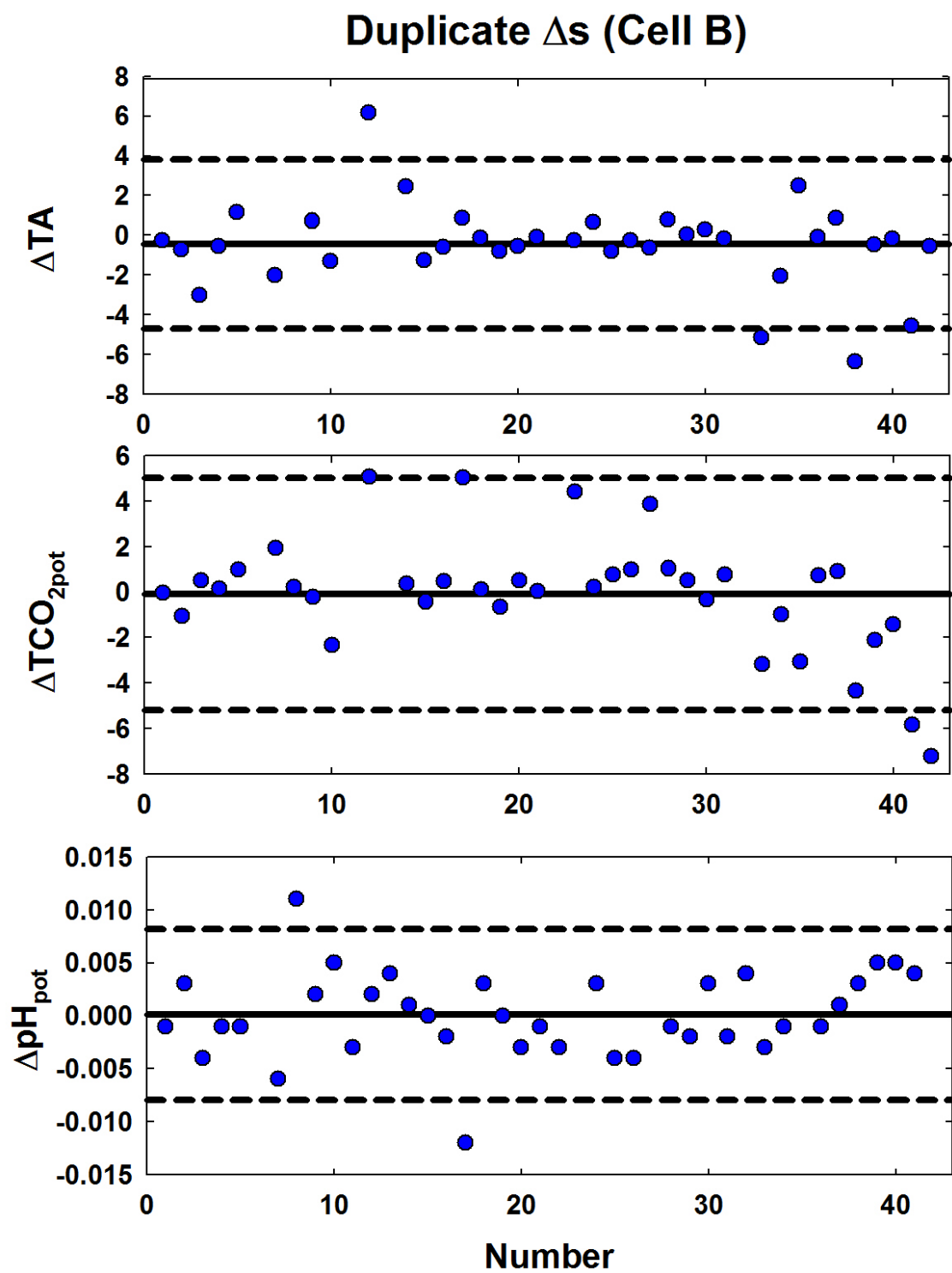


Figure 6. The reproducibility of TA ($\mu\text{mol}\cdot\text{kg}^{-1}$), TCO_{2pot} ($\mu\text{mol}\cdot\text{kg}^{-1}$), and pH_{pot} on Cell B. The dashed lines are 2 standard deviations from the means (solid lines).

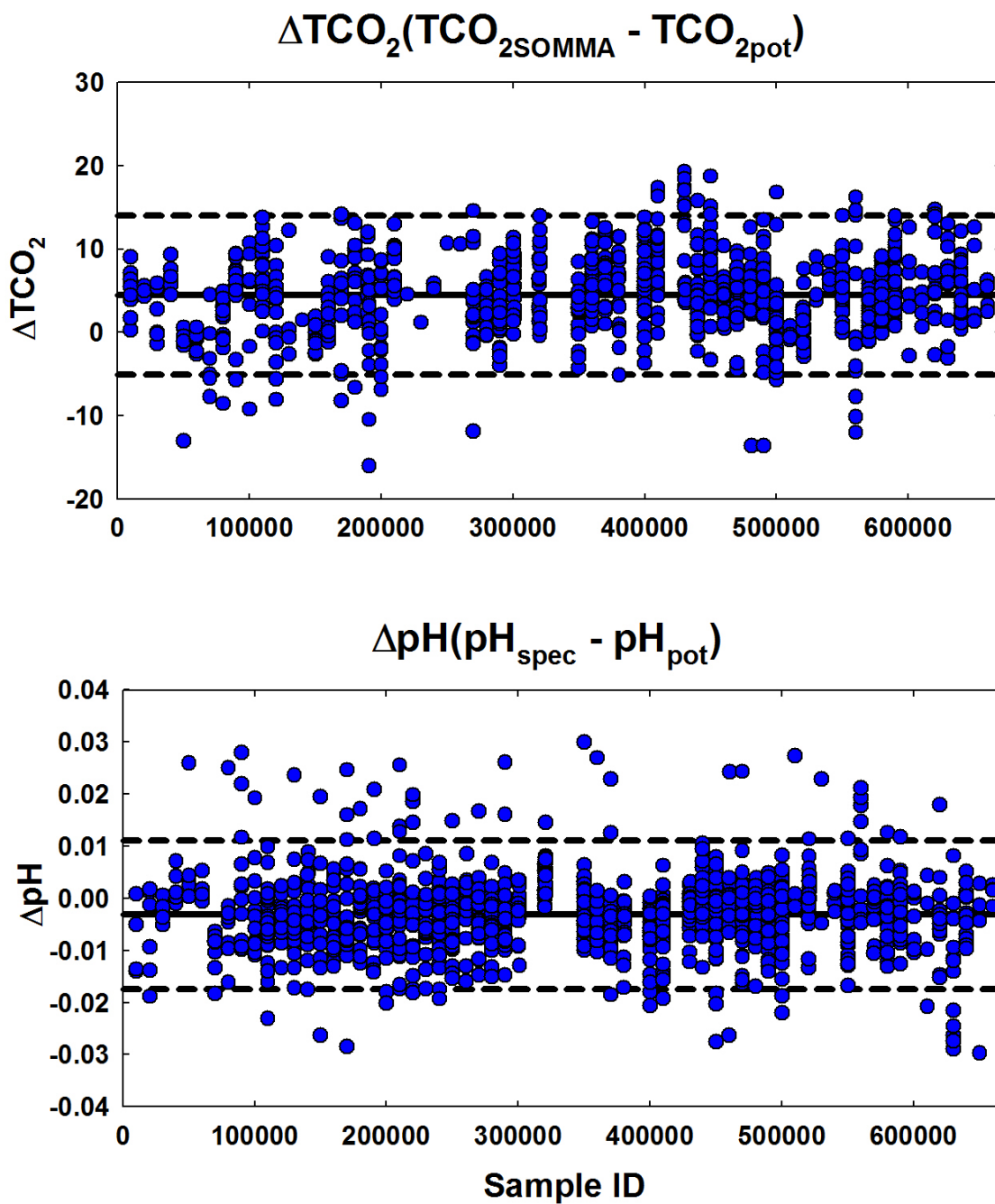


Figure 7. Difference between the TCO_2 ($\mu\text{mol}\cdot\text{kg}^{-1}$) measured by SOMMA and potentiometry (top), and the difference between pH measured by spectrophotometry and potentiometry (bottom). The dashed lines are 2 standard deviations from the means (solid lines).

3.2 Coulometric TCO₂ Accuracy and Precision:

A total of 953 unique samples were collected and analyzed for TCO₂. Of those, 7.5% were duplicates, and 5.7% were flagged as bad or questionable. The reproducibility of the coulometric TCO₂ SOMMA system was monitored throughout the cruise by making measurements on CRMs and duplicates of the same sample. CRMs were run on each new coulometric cell at least once before running any samples. The mean and standard deviation of the difference between the measured value and the certified value was -2.20 ± 2.45 (N = 61) and are shown in figure 8. At the end of station 45 tubing had to be replaced on valves 4 and 5, which could potentially change the volume of the pipette. This can be seen as a small increase in the average measured CRM value after station 45.

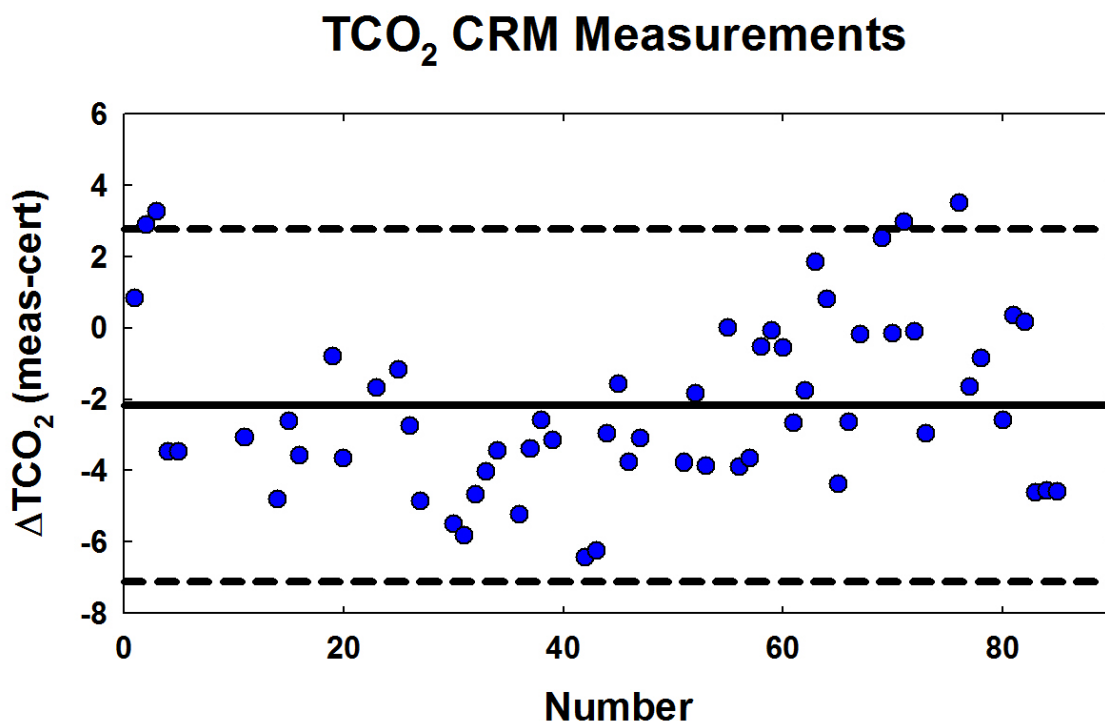


Figure 8. Difference between measured TCO₂ ($\mu\text{mol}\cdot\text{kg}^{-1}$) and certified value of CRM. Dashed lines are 2 standard deviations from the mean (solid line).

During repeat hydrography stations 3 duplicates were measured, one collected near the surface, one near the O₂ minimum, and one in the deep waters. When samples from a single station were analyzed on more than one cell at least one duplicate was analyzed on each cell whenever possible. The mean and standard deviation of the duplicates was -0.21 ± 2.77 (N = 73) and are shown in figure 9. These values are reasonable for this method, although the standard deviation may be slightly higher due to the conditions in the laboratory van being less stable than desirable (poor control of laboratory temperature and humidity).

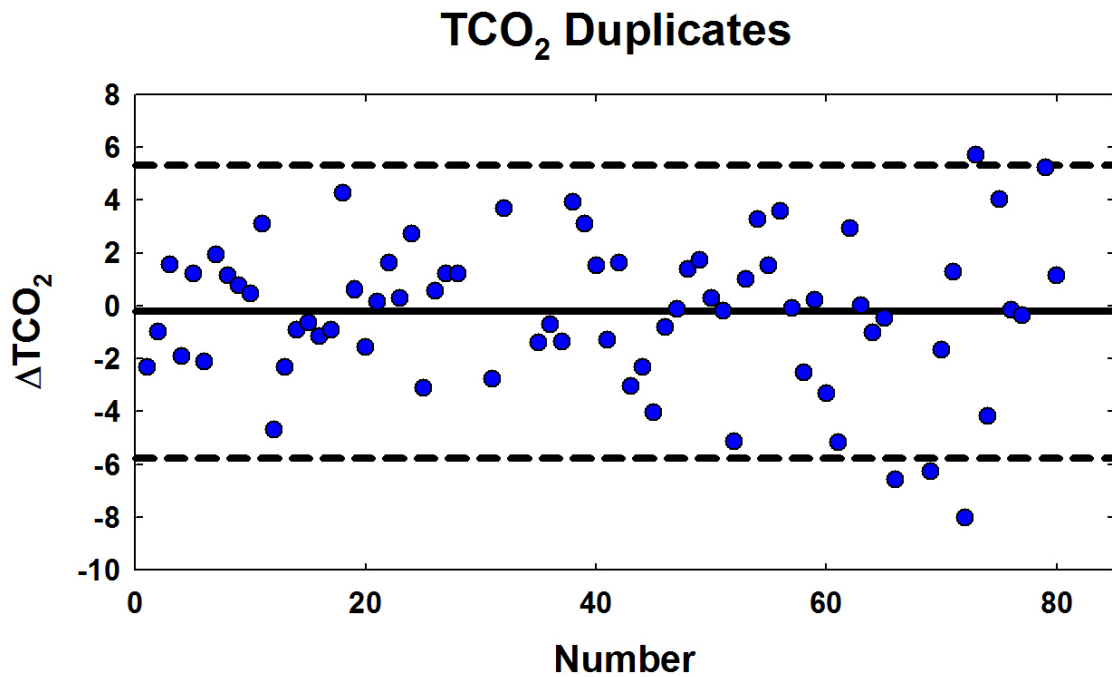


Figure 9. Duplicate measurements of TCO₂ (μmol·kg⁻¹) measured on the SOMMA instrument. Dashed lines are 2 standard deviations from the mean (solid line).

3.3 Discrete pH Accuracy and Precision

A total of 1,266 unique samples were analyzed for pH. Of those, 4.5% were duplicates, and 6.5% were flagged as questionable or bad. The main cause for a bad value was a bubble in the cell while taking absorption measurements. The low percentage of duplicates is the result of water budget restrictions preventing duplicates from being taken on GEOTRACES stations. The reproducibility of the spectrophotometric pH system was monitored throughout the cruise by making measurements on CRM, TRIS buffer, and duplicates of the same sample (table 4). The differences between the duplicates are shown in figure 10. All values have been corrected to exactly 25°C (see section 1.2.3).

Table 4. Accuracy and precision of spectrophotometric pH measurements using CRM, TRIS buffer, and duplicate measurements.

	pH	Δ^a
CRM	7.8987 ± 0.0039 N = 31	-0.0058 ± 0.0039 N = 31
TRIS^b	8.0975 ± 0.0049 N = 37	0.0049 ± 0.0049 N = 37
Duplicates		0.0004 ± 0.0023 N = 55

^aRelative to the calculated value for CRM and TRIS, Duplicates are first - second replicate

^bTRIS is measured on the total scale since no F is present

Measurements were made on the TRIS buffer in the lab before the cruise, and had a mean and standard deviation of 8.0965 ± 0.0013 (N = 9), which is in good agreement with the value measured during the cruise. The agreement between pre-cruise and cruise

TRIS measurements demonstrates that biological growth that occurred in some of the TRIS bottles did not adversely impact the pH. The precision of the CRM, TRIS, and duplicates are comparable to those determined on previous cruises. The mean of the duplicates being so close to zero demonstrates that no significant gas exchange occurs between collection and analysis of the samples.

Spectrophotometric pH Duplicates

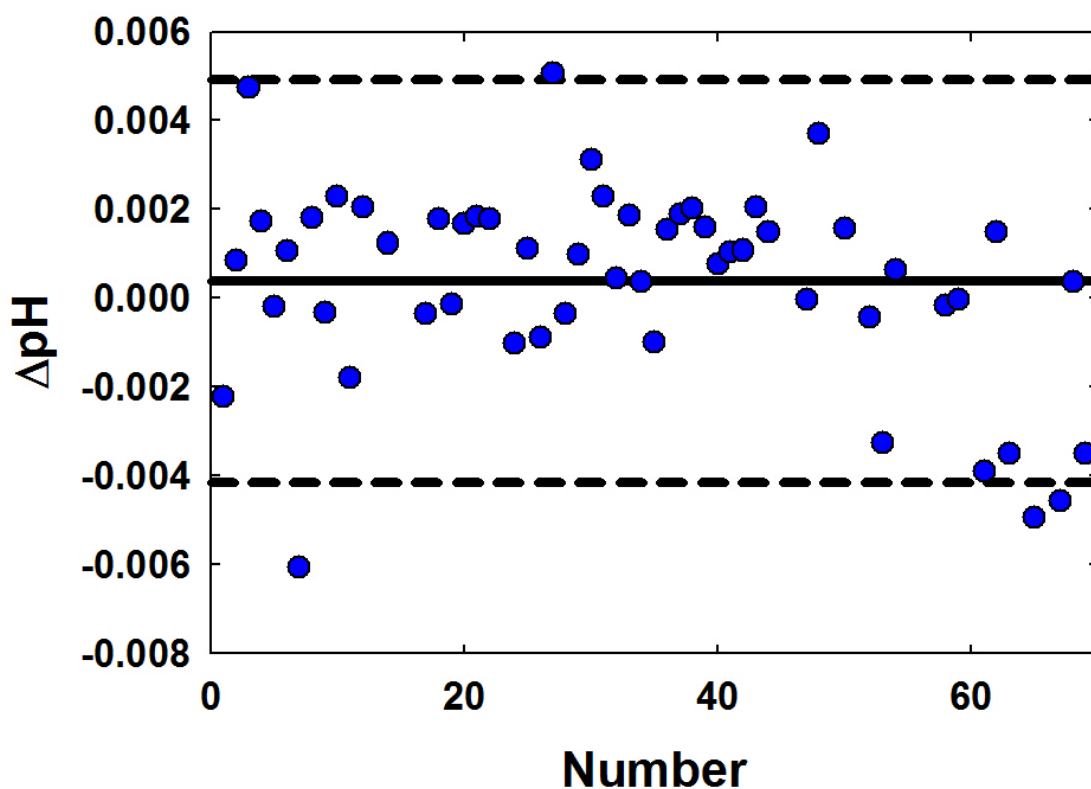


Figure 10. Precision of spectrophotometric pH measurements using duplicates (1st measurement - 2nd measurement). The dashed lines are 2 times the standard deviation from the mean (solid line).

As discussed earlier, the pH was also obtained from the less precise potentiometric pH titration. The two values were compared and the differences are shown in figure 11. The mean and standard deviation is -0.0031 ± 0.0071 ($N = 1226$).

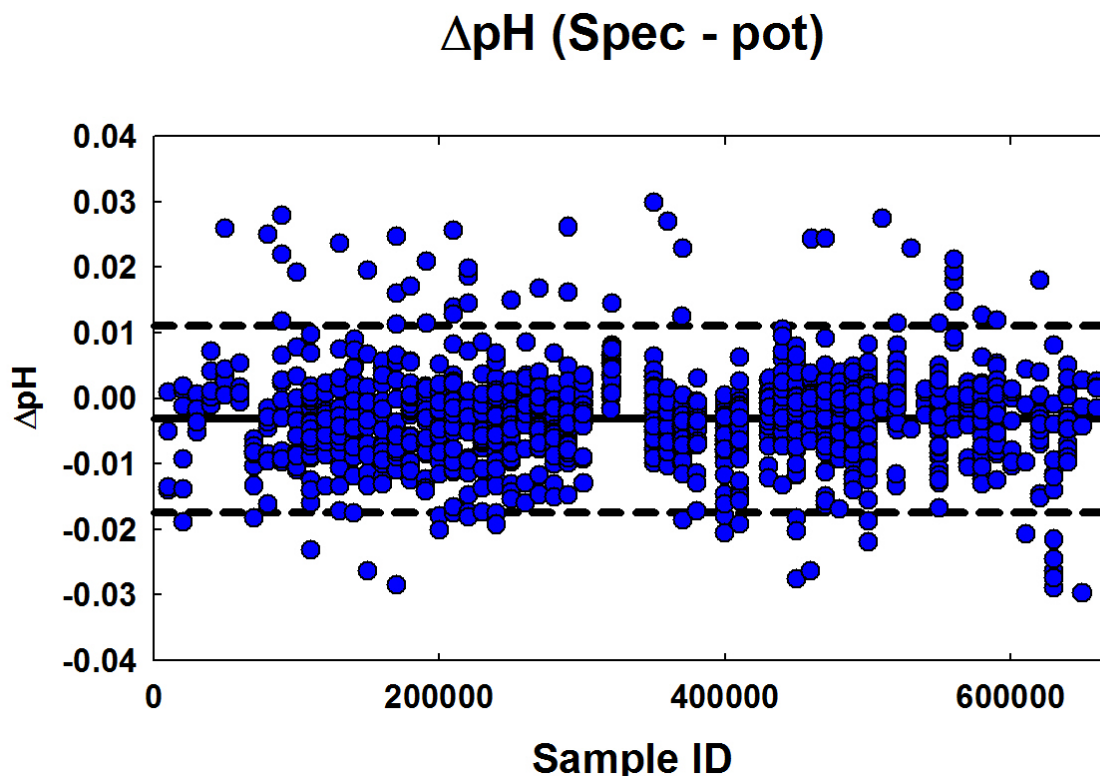


Figure 11. Difference between the pH measured by spectrophotometry and potentiometry. The dashed lines are 2 standard deviations from the mean (solid line).

4. Internal Consistency

The carbonate system is characterized by four parameters: TA, TCO_2 , pCO_2 and pH. Knowing two of these parameters, the other two can be calculated. If more than two parameters are known, the system is overdetermined and a comparison of calculated and measured values can be used to examine the internal consistency of the system. We have examined the internal consistency of our pH, TA and TCO_2 measurements. We used the Excel version 2.1 of CO_2sys program (Pierrot *et al.*, 2006) using the carbonic acid

constants of Millero (2006) and Borate concentrations of Lee *et al.* (2010) for all calculations.

The results of these calculations are summarized in table 5 and the deviations are shown in figure 12. The calculated values of ΔTA and ΔTCO_2 are all reasonable with standard deviations near $\pm 5 \mu\text{mol}\cdot\text{kg}^{-1}$. The calculated values of ΔpH are similarly reasonable with a standard deviation below ± 0.015 . The values are all comparable to other studies, although likely a little higher than would have been, due to the non-ideal conditions of the lab van.

Table 5. Difference between the measured and calculated values of TA, TCO_2 , and pH.

Parameter	Input	Mean	Stdev	Number
ΔTA	pH, TCO_2	-0.88	5.41	889
ΔTCO_2	TA, pH	0.85	5.27	889
ΔpH	TA, TCO_2	0.0021	0.0147	889

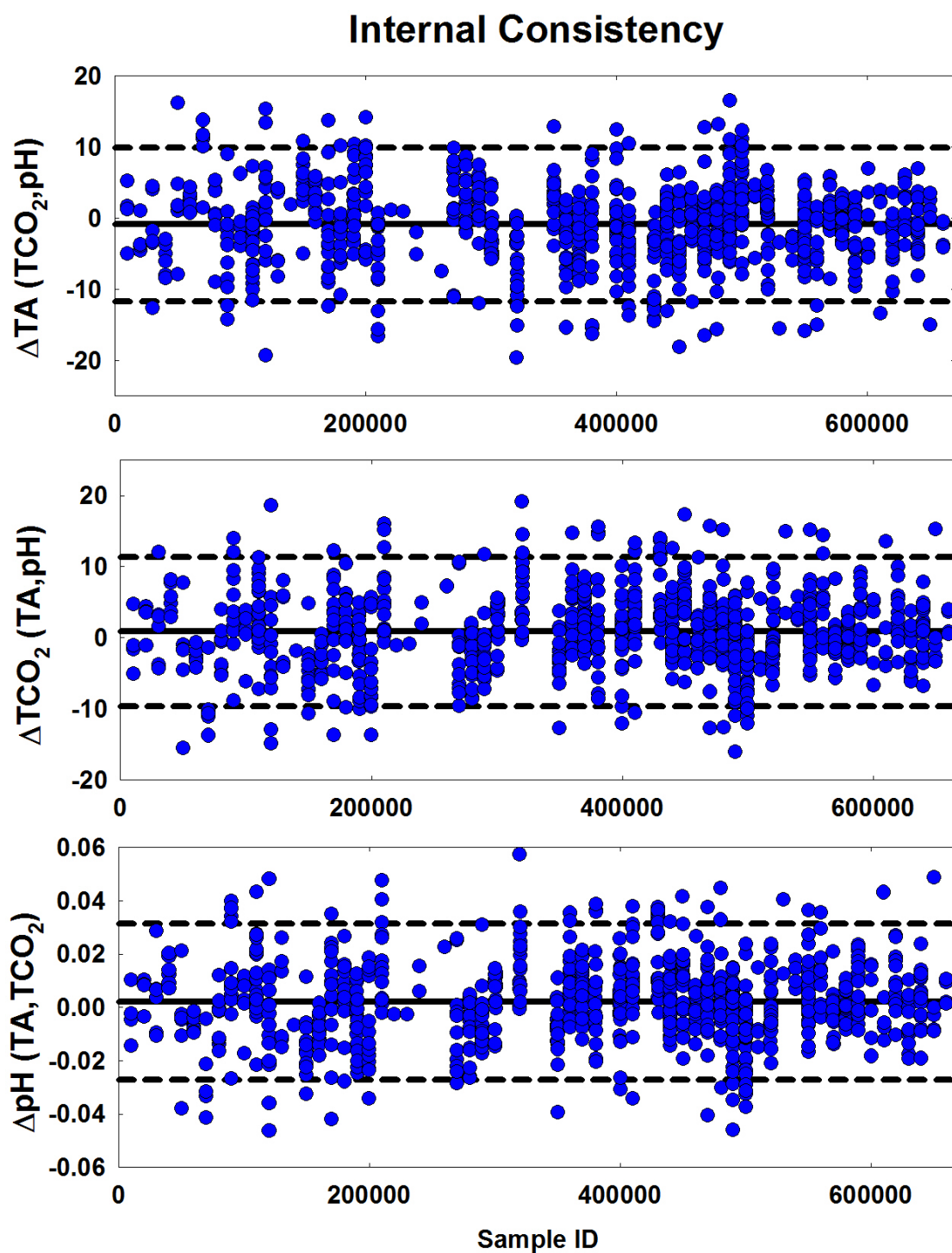


Figure 12. Difference between the measured and calculated values of TA, TCO_2 , and pH. The input variables for the calculated values are shown in parentheses. The dashed lines are 2 standard deviations from the means (solid lines).

5. Distribution of the Carbon Parameters in Seawater Along the ARC01 Track

Sections showing the distribution of TA (figure 13), TCO₂ (figure 14), and pH (figure 15) are shown below. All sections were made using Ocean Data View version 4.7.7 (Schlitzer, 2016). Each figure is divided into four different panels. The top panels show the surface to a depth of 100 db, and the bottom panels show the deep waters from 100 db to the bottom. The northward section in the Makarov basin is shown on the left-hand panels and the southward section in the Canada Basin is shown in the right-hand panels. The panels are centered on the North Pole. Stations 1-6 are not shown because they are located in the Pacific Ocean. Low values of TA and TCO₂ are found in the surface waters due to dilution from ice melt and river water inputs, and deep waters are similar to their Atlantic source water. Surface pH is low compared to surface Atlantic or Pacific waters, with a minimum found around 60-100 db. Deep waters are similar to North Atlantic deep water.

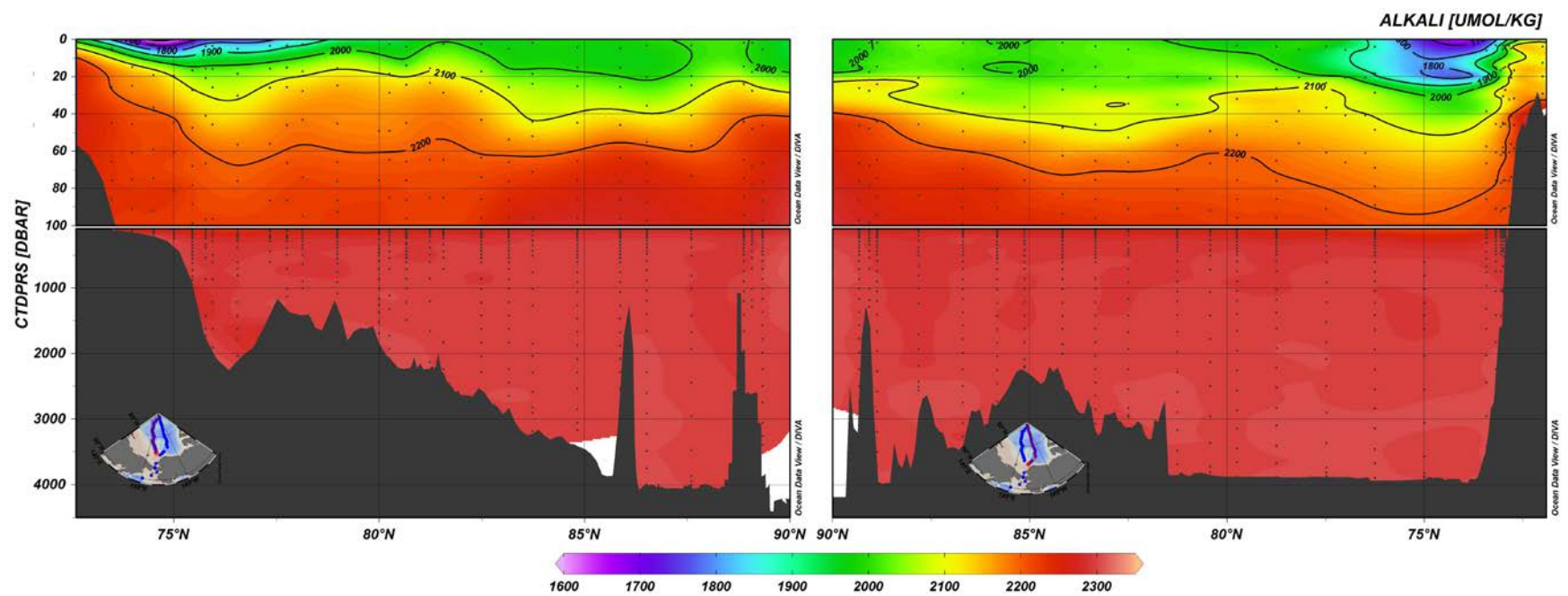


Figure 13. Measured TA in $\mu\text{mol}\cdot\text{kg}^{-1}$. Left panels show the Makarov Basin section from south to north (left to right), and right panels show the Canada Basin section from north to south (left to right).

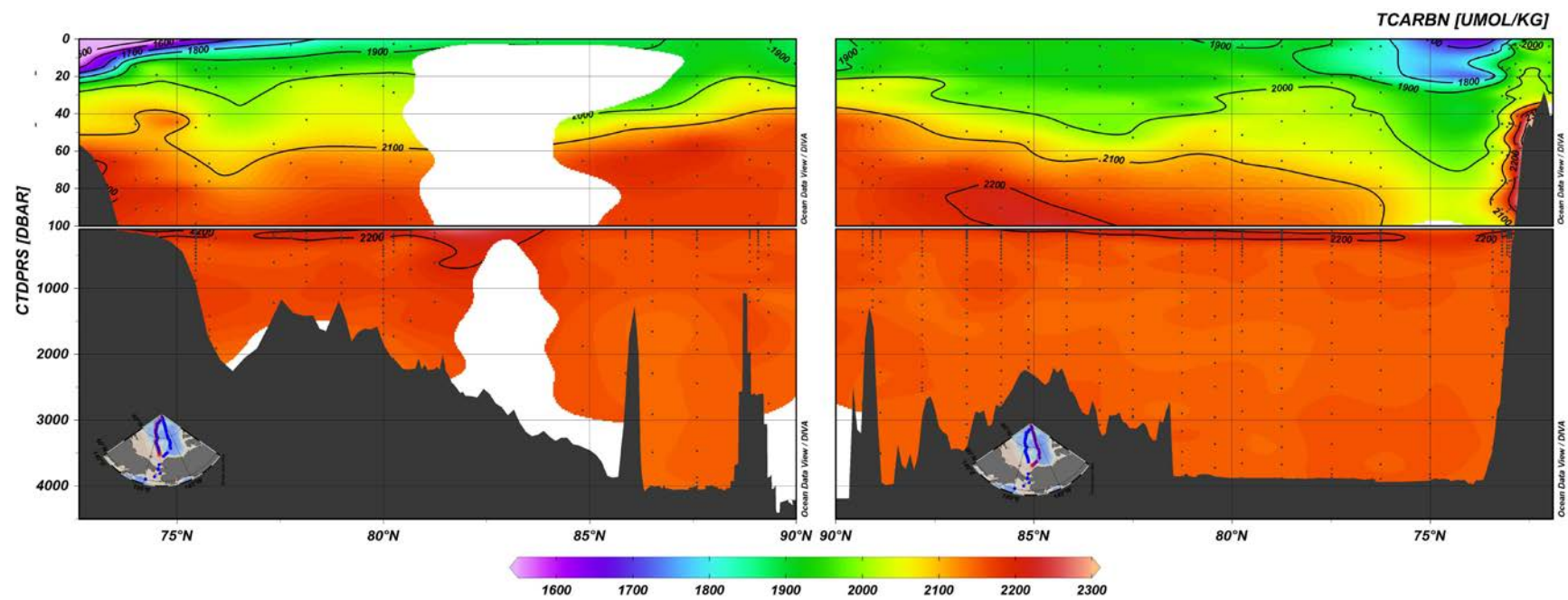


Figure 14. Measured TCO_2 in $\mu\text{mol}\cdot\text{kg}^{-1}$. Left panels show the Makarov Basin section from south to north (left to right), and right panels show the Canada Basin section from north to south (left to right).

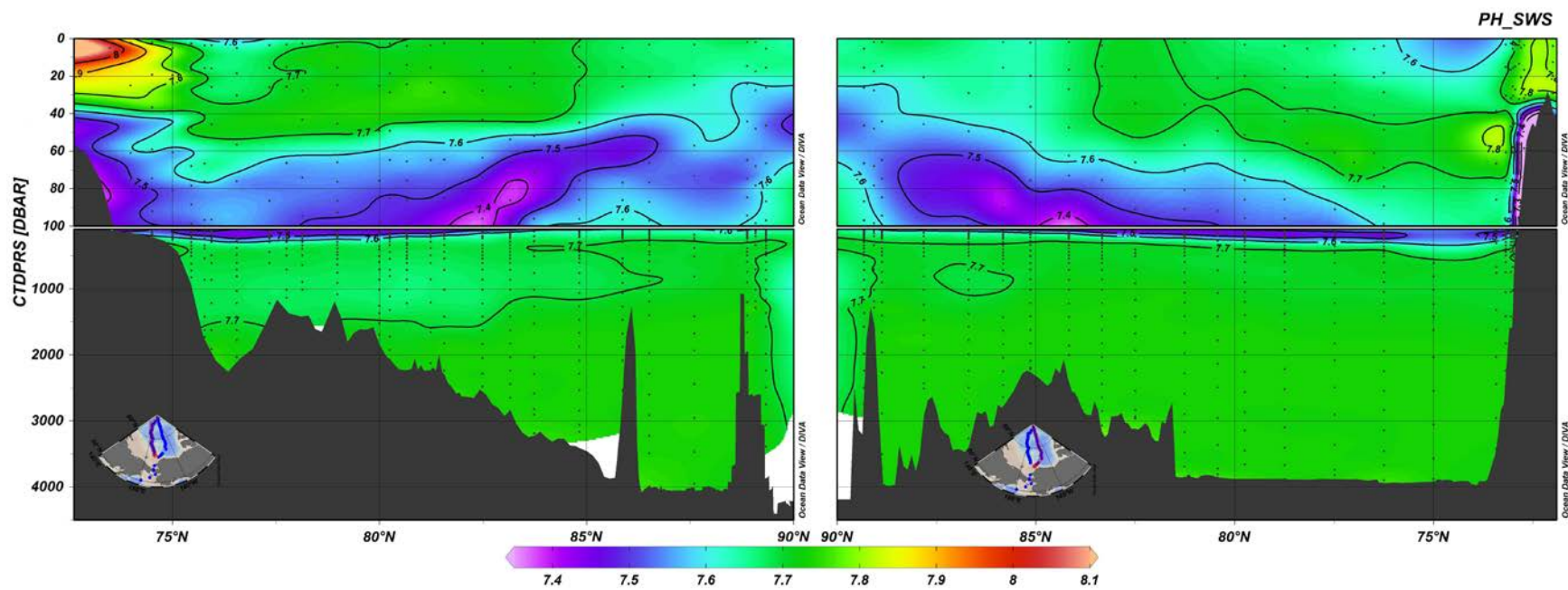


Figure 15. Measured pH at 25°C. Left panels show the Makarov Basin section from south to north (left to right), and right panels show the Canada Basin section from north to south (left to right).

6. Decadal Changes in Carbon Parameters (1994-2015)

The cruise track was designed to be repeat occupations of previous cruises in order to observe changes in physical chemical parameters. The northward segment along the Makarov Basin was a repeat of the AOS94 cruise completed by Canada aboard the R/V *Louis S. St-Laurent*. The southward segment along the Canada Basin was a repeat of the CLIVAR AOS05 cruise completed by Sweden aboard the R/V *Oden*. Based on recommendations from GLODAP version 2, a correction of $-29 \mu\text{mol}\cdot\text{kg}^{-1}$ was made to the TA, and corrections factors of 0.9 and 1.05 were applied to silicate and CFC-11 respectively for the AOS94 cruise (Key *et al.*, 2015). Based on comparisons with our data and internal consistency calculations, the GLODAP version 2 corrections for AOS05 (Key *et al.*, 2015) were not applied (see section 6.2 for more details). On AOS05 the pH was measured at 15°C, and has been corrected to 25°C using TA and CO2sys, the difference in temperature is too large to use equation 6. The repeat sections allow us to look at changes in the chemical parameters over 10 and 20 year time periods. Comparisons of changes in the chemical parameters are discussed in the sections below.

The ARC01 cruise track was not an exact repeat of the previous cruises. Most notably the AOS05 cruise had to go around the Alpha ridge due to thick ice, moving the cruise track closer to Russia, compared to the ARC01 cruise. The AOS05 also continued nearly all the way to the Alaska coast, instead of turning towards the Bering Strait at $\sim 75^\circ\text{N}$ as the ARC01 cruise did.

6.1 Changes in Surface Measurements

The surface is the area most likely to experience large changes over decadal time scales. The mixed layer is most variable to do seasonal variations, interactions with the atmosphere, and variability in circulation and biological activity. The mixed layer was determined to be, on average, about 40 db over the entire cruise track. The salinity of the mixed layer for all three occupations is shown in figure 16. Large decreases of greater than 1 are seen in the salinity across the entire cruise track. This is likely caused mainly by increased ice melt, but also potentially from increased input of freshwater from rivers. The increased scatter in the ARC01 data compared to AOS94 indicates a decrease in the mixed layer south of $\sim 84^{\circ}\text{N}$ between the two occupations. The surface oxygen measurements are shown in figure 17. There may be a slight increase in O_2 between 1994 and 2015, but there is no obvious difference between 2005 and 2015.

The carbon parameters show large differences between the occupations. TA (figure 18) has a large decrease over the last 10 and 20 years. To account for dilution from ice melt the TA is normalized to a salinity of 35 (NTA; figure 19). The NTA shows increases over the last two decades indicating a source of alkalinity either from ice melt or river input. The changes in TCO_2 (figure 20) and normalized TCO_2 (NT CO_2 ; figure 21) show very similar patterns to TA and NTA, respectively. The changes in both TA and TCO_2 are much larger than would be expected by uptake of atmospheric CO_2 indicating other changes in the Arctic, principally ice melt, are driving the changes. The pH was not measured on AOS94; however, the pH between AOS05 and ARC01 is shown in figure 22. The pH shows a large decrease between 2005 and 2015.

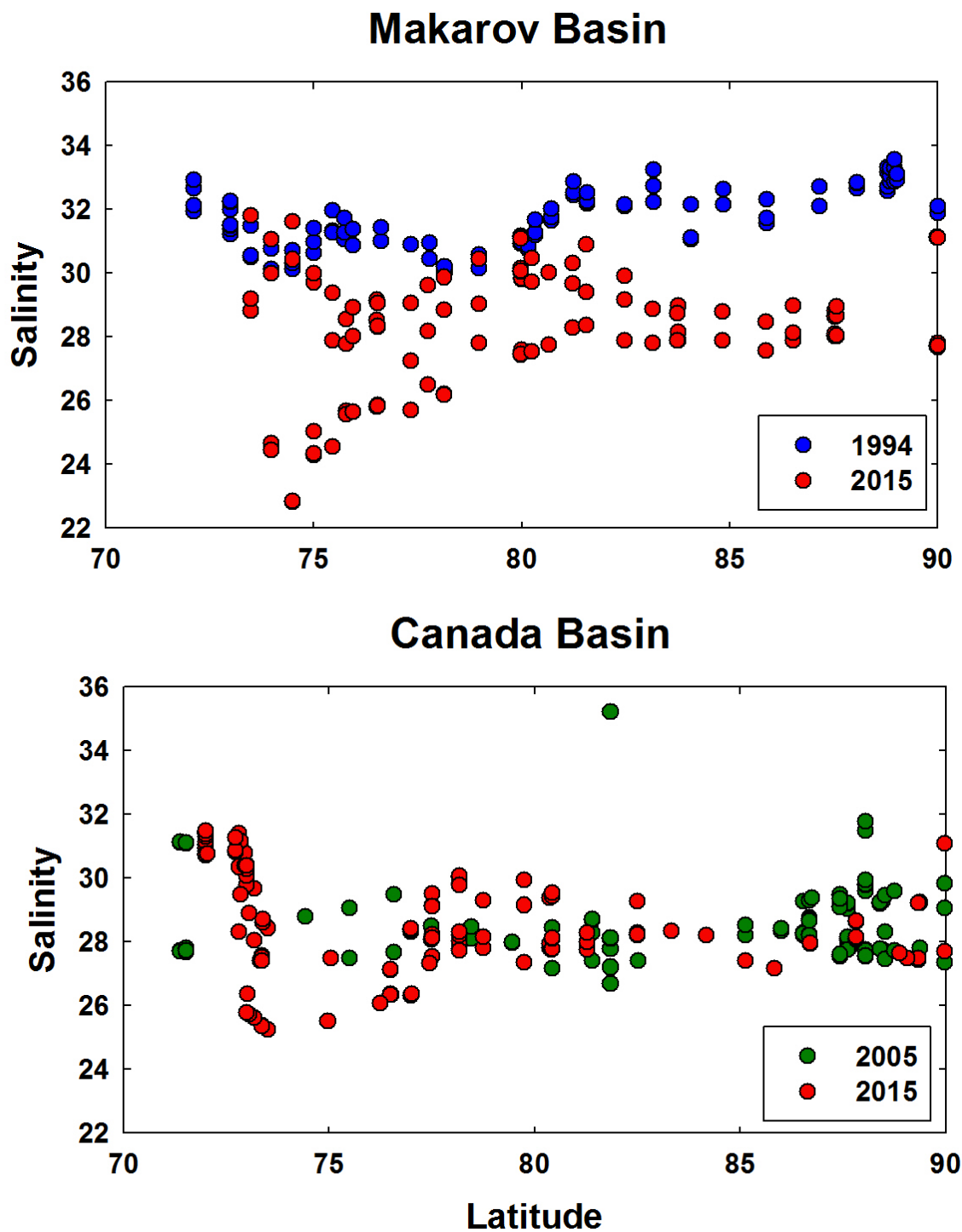


Figure 16. Comparison of the surface (<40 db) salinity between the AOS94 and ARC01 cruises in the upper panel, and AOS05 and ARC01 cruises in the lower panel.

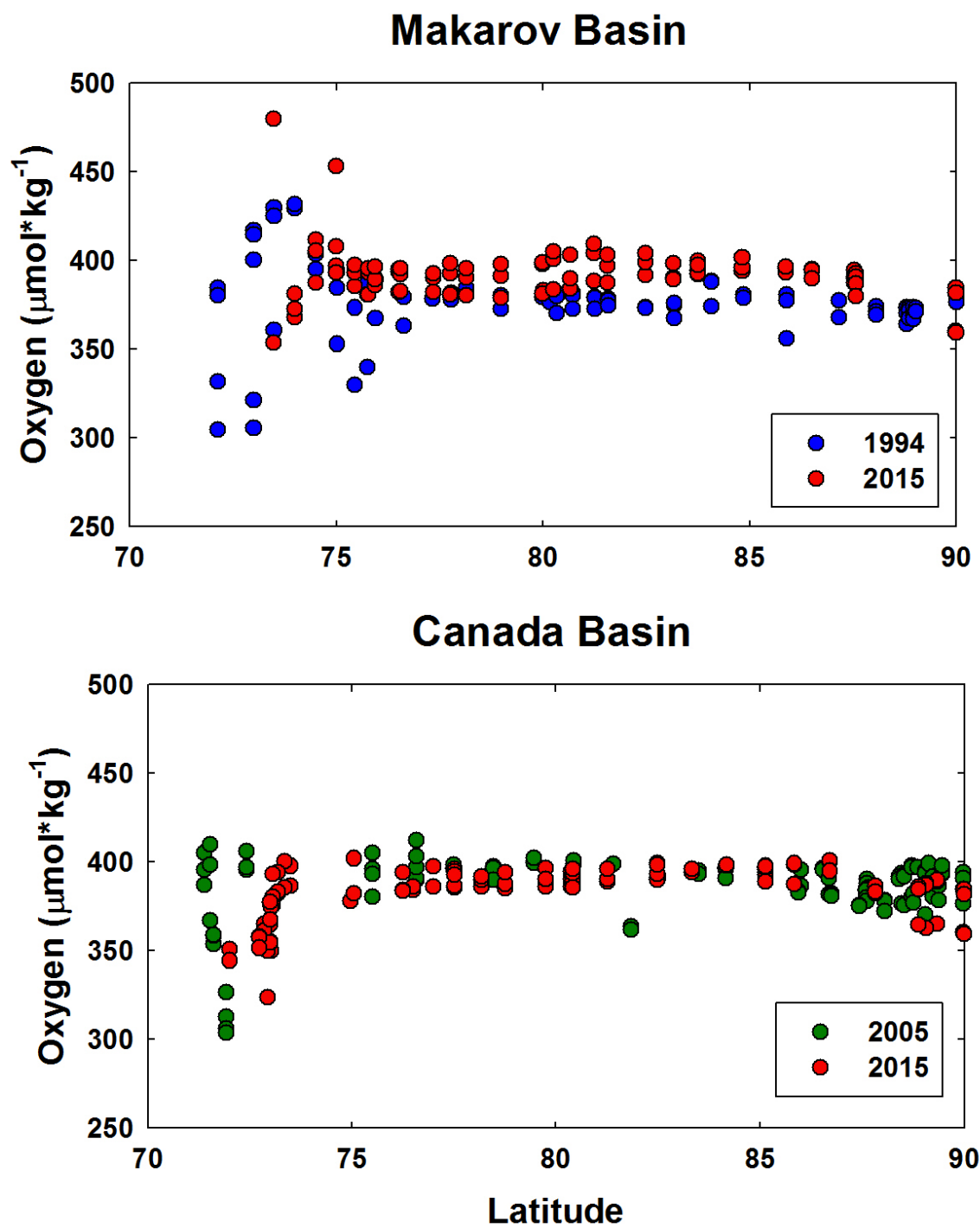


Figure 17. Comparison of the surface (<40 db) oxygen between the AOS94 and ARC01 cruises in the upper panel, and AOS05 and ARC01 cruises in the lower panel.

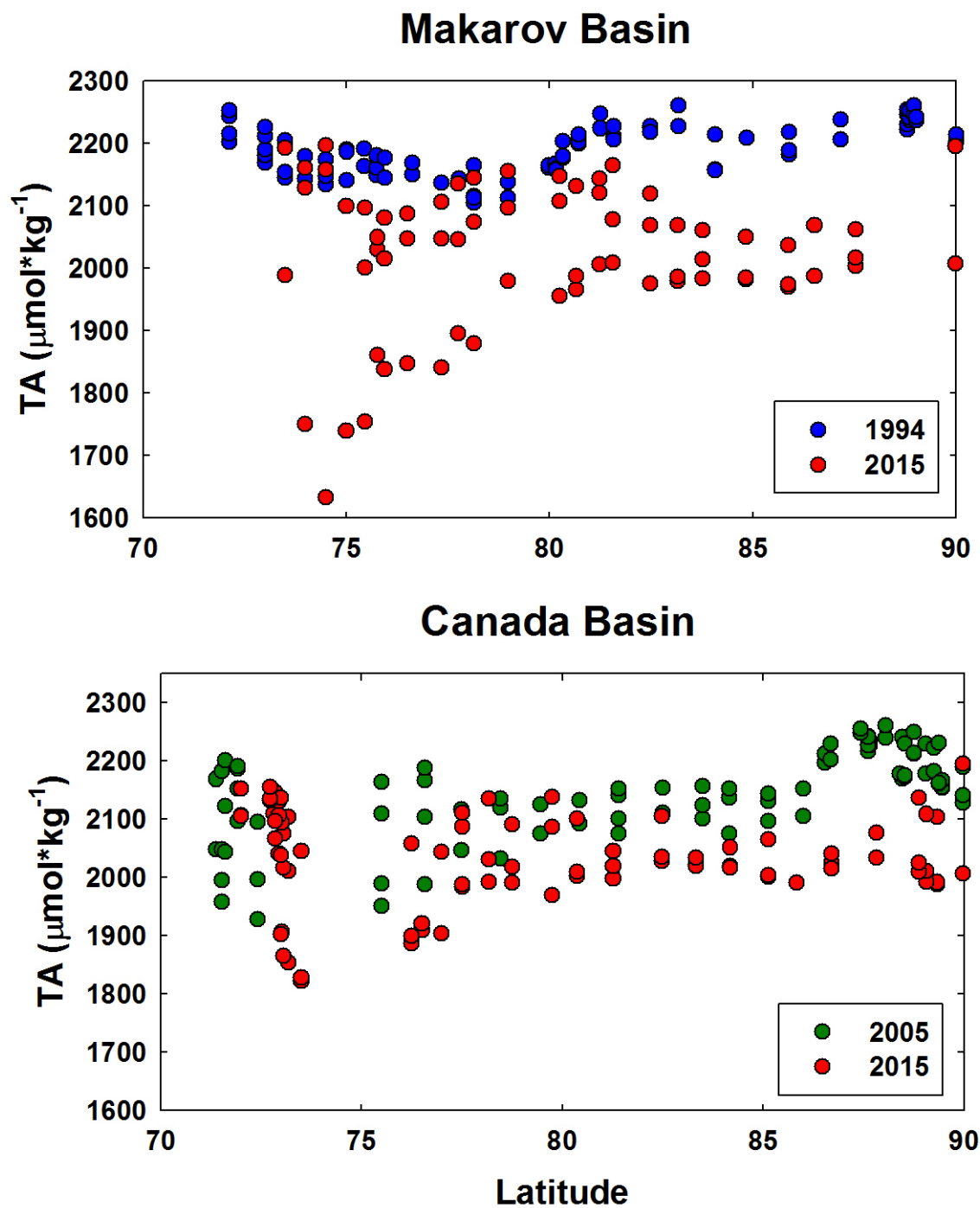


Figure 18. Comparison of the surface (<40 db) TA between the AOS94 and the ARC01 cruises in the upper panel, and the AOS05 and ARC01 cruises in the lower panel.

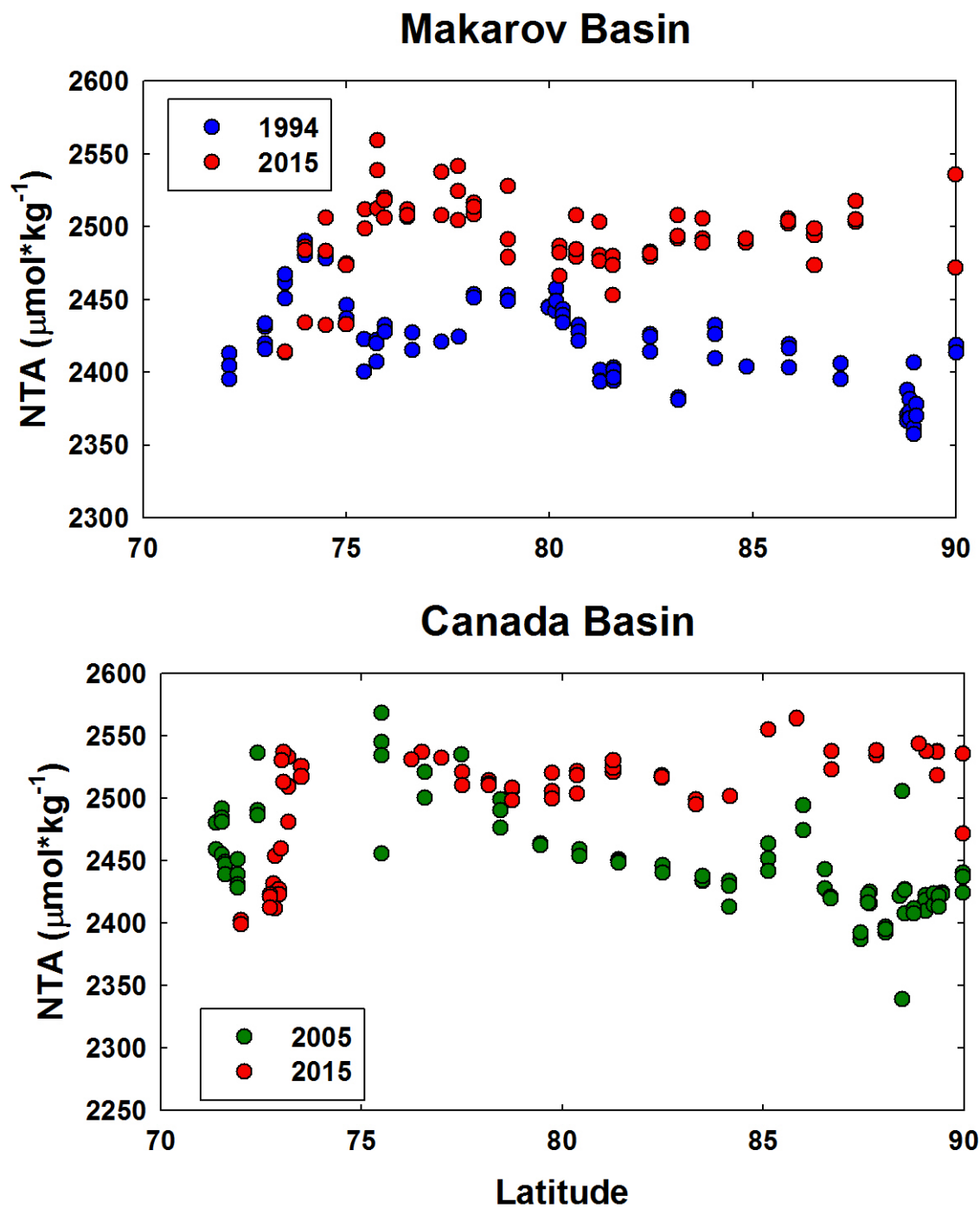


Figure 19. Comparison of the surface (<40 db) NTA between the AOS94 and ARC01 cruises in the top panel, and the AOS05 and ARC01 cruises in the bottom panel.

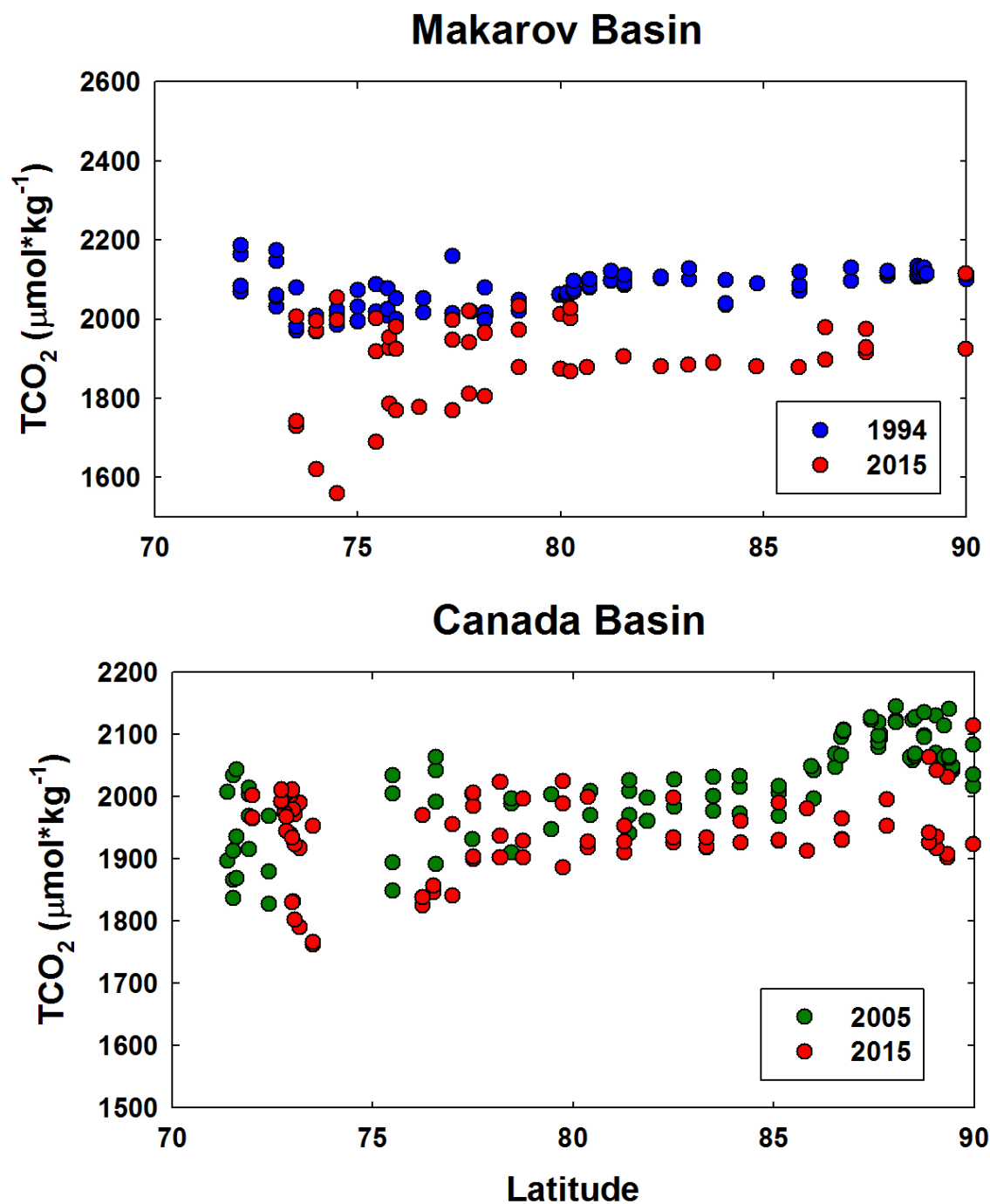


Figure 20. Comparison of the surface (<40 db) TCO_2 between the AOS94 and the ARC01 cruises in the upper panel, and the AOS05 and ARC01 cruises in the lower panel.

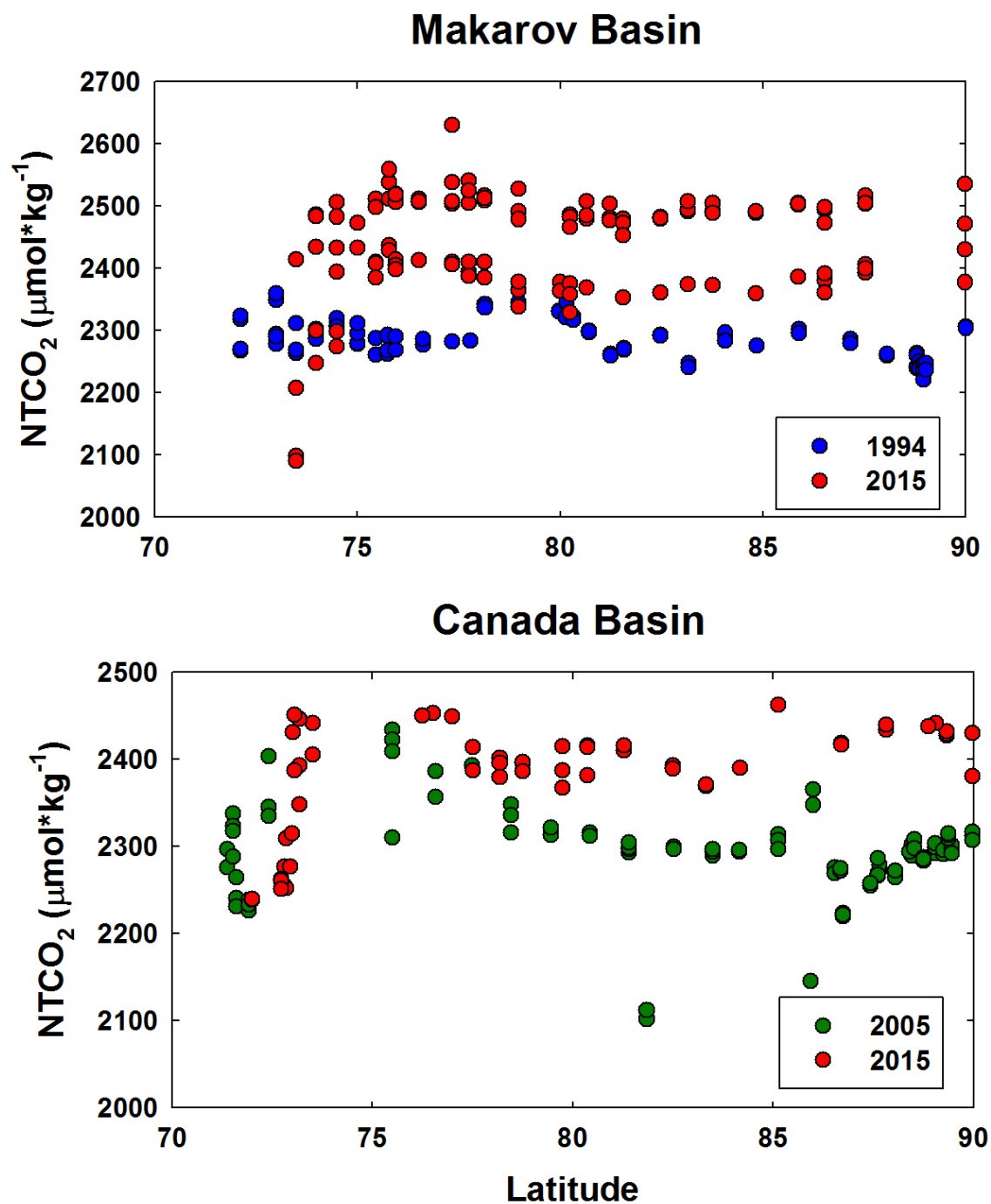


Figure 21. Comparison of the surface (<40 db) NTCO₂ between the AOS94 and ARC01 cruises in the top panel, and the AOS05 and ARC01 cruises in the bottom panel.

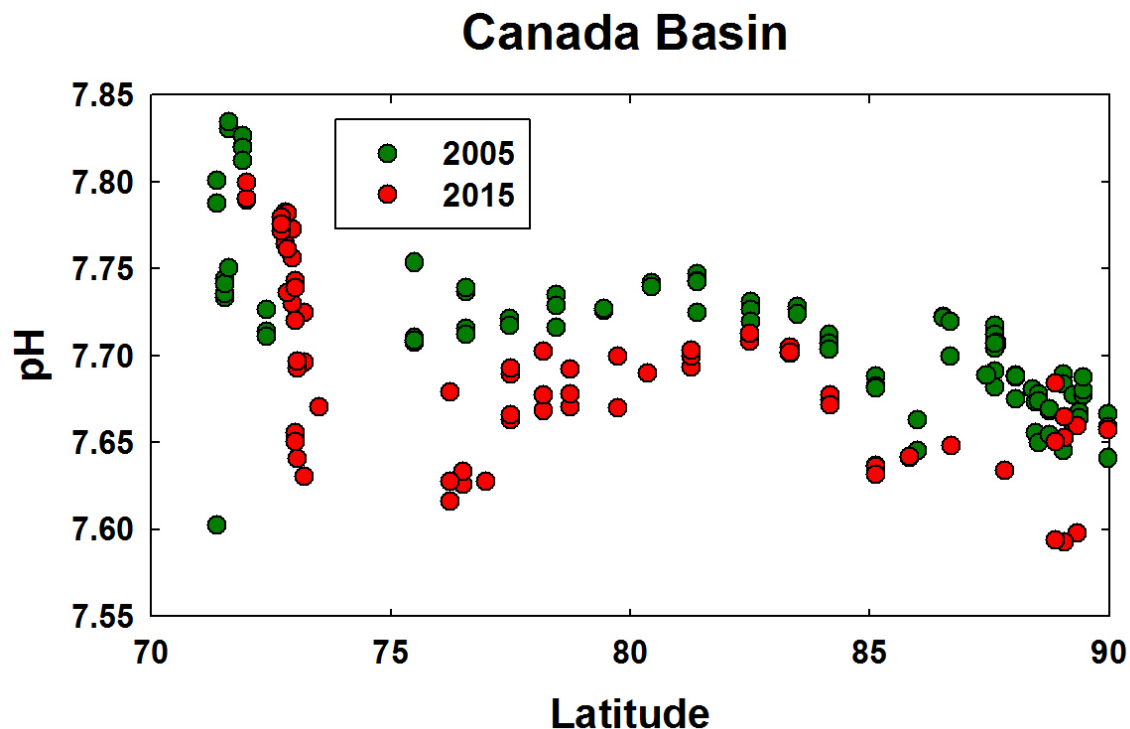


Figure 22. Comparison of the surface (<40 db) pH at 25°C between the AOS-2005 and ARC01 cruises. The AOS05 data were measured at 15°C and were corrected to 25°C using TA and CO₂sys.

6.2 Changes Between the AOS 2005 and the GO-SHIP ARC01 2015

Changes in TA between the 2005 and 2015 occupations are shown in figure 23. The difference (ARC01-AOS05) between the deep waters (>2000 m) have a mean and standard deviation of $3.1 \pm 2.8 \mu\text{mol}\cdot\text{kg}^{-1}$, which is similar to the accuracy of the measurements. There are large decreases of over $200 \mu\text{mol}\cdot\text{kg}^{-1}$ in the surface waters. As can be seen in figure 16, there are also significant changes in salinity. To account for these changes, the NTA is shown in figure 24. The upper 500 m shows significant increases in NTA, indicating that ice melt (or increased river input) contains a significant amount of alkalinity.

GLODAP version 2 (Key *et al.*, 2015) recommends a correction of $-5 \mu\text{mol}\cdot\text{kg}^{-1}$ for AOS05 TCO_2 . Then, based on internal consistency calculations, a correction of -0.017 for pH. Applying these corrections results in unexpectedly large changes in waters deeper than 2000 m, $-12.8 \pm 10.9 \mu\text{mol}\cdot\text{kg}^{-1}$ for TCO_2 and 0.025 ± 0.012 pH units. If no correction is applied to the data, the difference in the deep waters is $-17.8 \mu\text{mol}\cdot\text{kg}^{-1}$ and 0.008 for TCO_2 and pH, respectively. The difference in pH is close to the uncertainty, especially with the added uncertainty involved in adjusting them to the same temperature. Based on this comparison, no adjustment is applied to the pH. Using the pH and TA, the internal consistency of the AOS05 data was calculated in order to determine a correction factor of $-11.6 (\pm 8.6 \text{ stdev}) \mu\text{mol}\cdot\text{kg}^{-1}$ for TCO_2 .

Figure 25 shows that differences in deep values of TCO_2 are $-3.2 \pm 5.6 \mu\text{mol}\cdot\text{kg}^{-1}$, but surface values show decreases greater than $150 \mu\text{mol}\cdot\text{kg}^{-1}$. This is opposite and an order of magnitude larger than changes expected from the uptake of anthropogenic CO_2 . To account for changes due to melting ice, NTCO_2 is shown in figure 26. As with NTA, the surface shows increases in NTCO_2 indicating that melting ice contains some amount of TCO_2 . Figure 27 shows the changes in pH between the 2 occupations. There are large changes in the surface waters. Decreases are much larger than would be expected from uptake of anthropogenic carbon, and some areas show large increases. The carbon system in the Arctic is more complicated than other oceans.

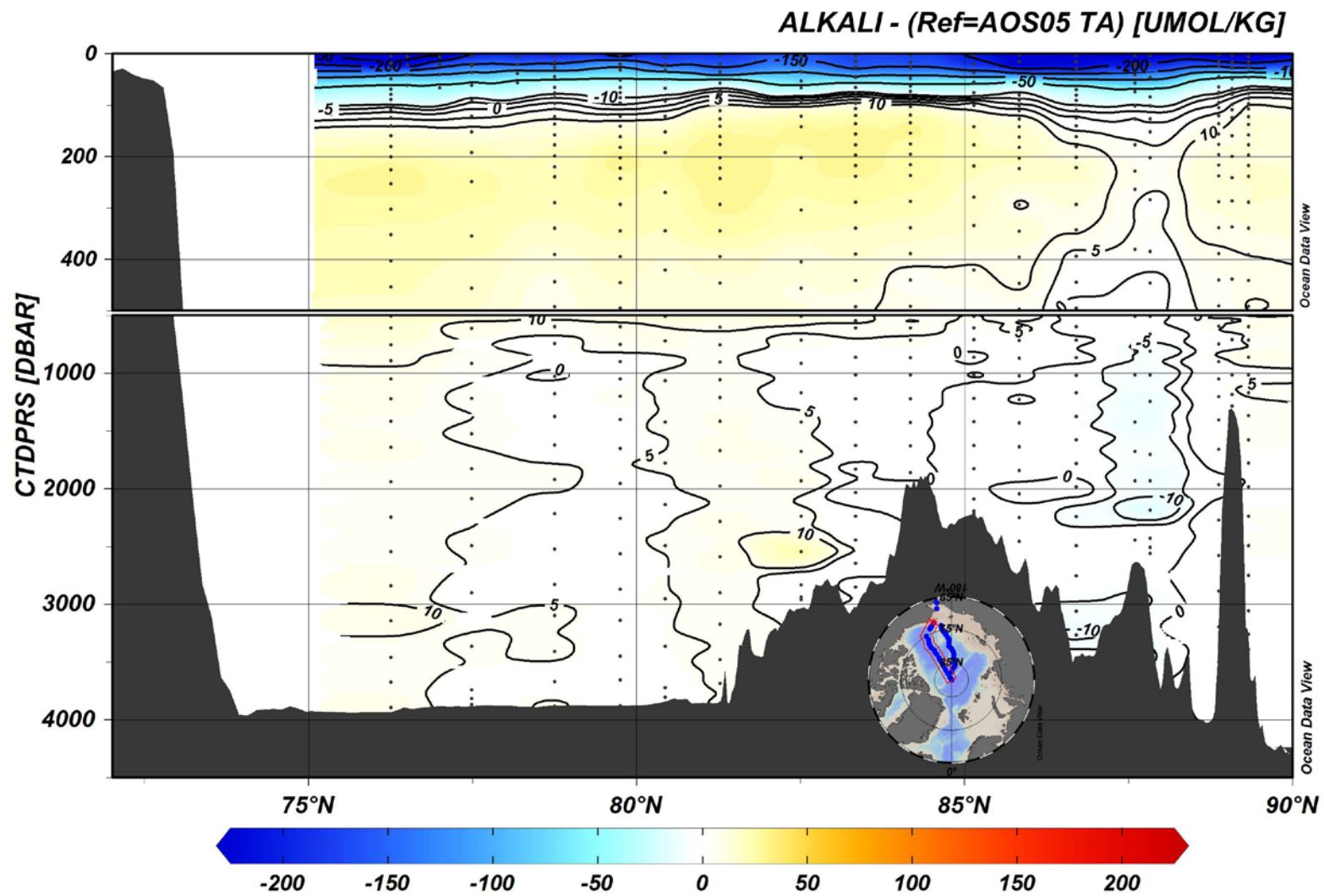


Figure 23. Changes in TA between the 2005 and 2015 occupations of the Canada Basin section.

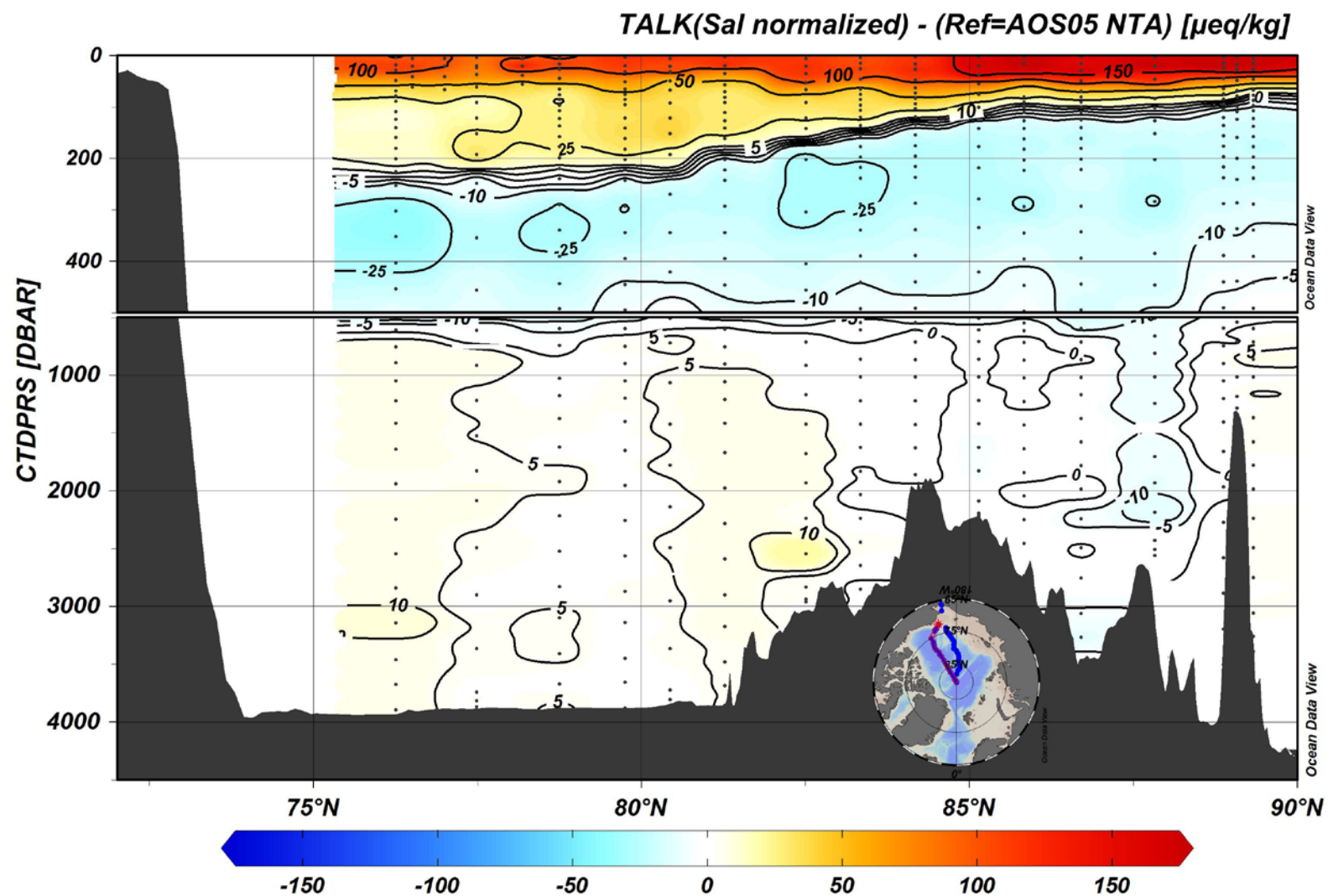


Figure 24. Changes in NTA between the 2005 and 2015 occupations of the Canada Basin.

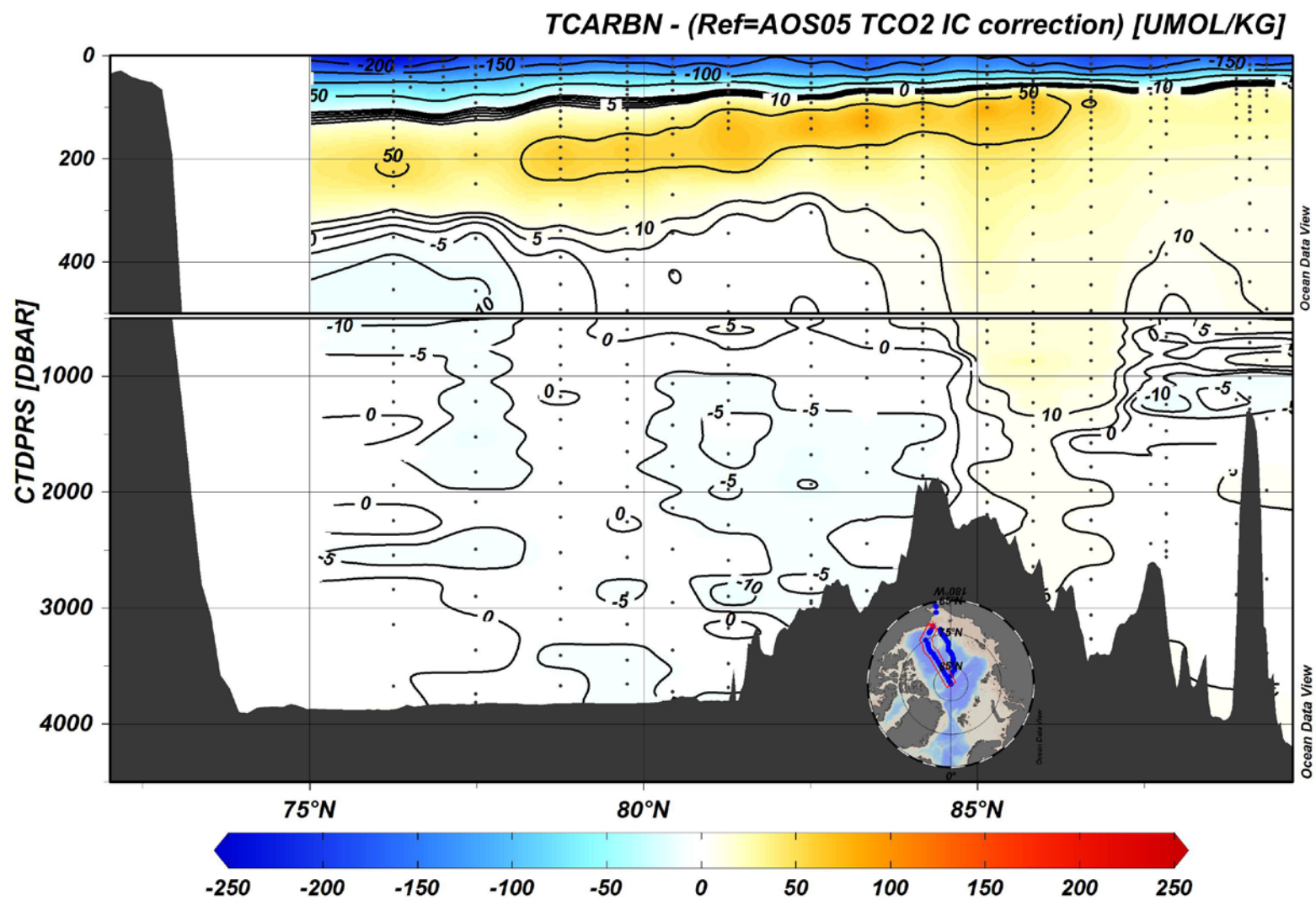


Figure 25. Changes in TCO₂ between the 2005 and 2015 occupations of the Canada Basin.

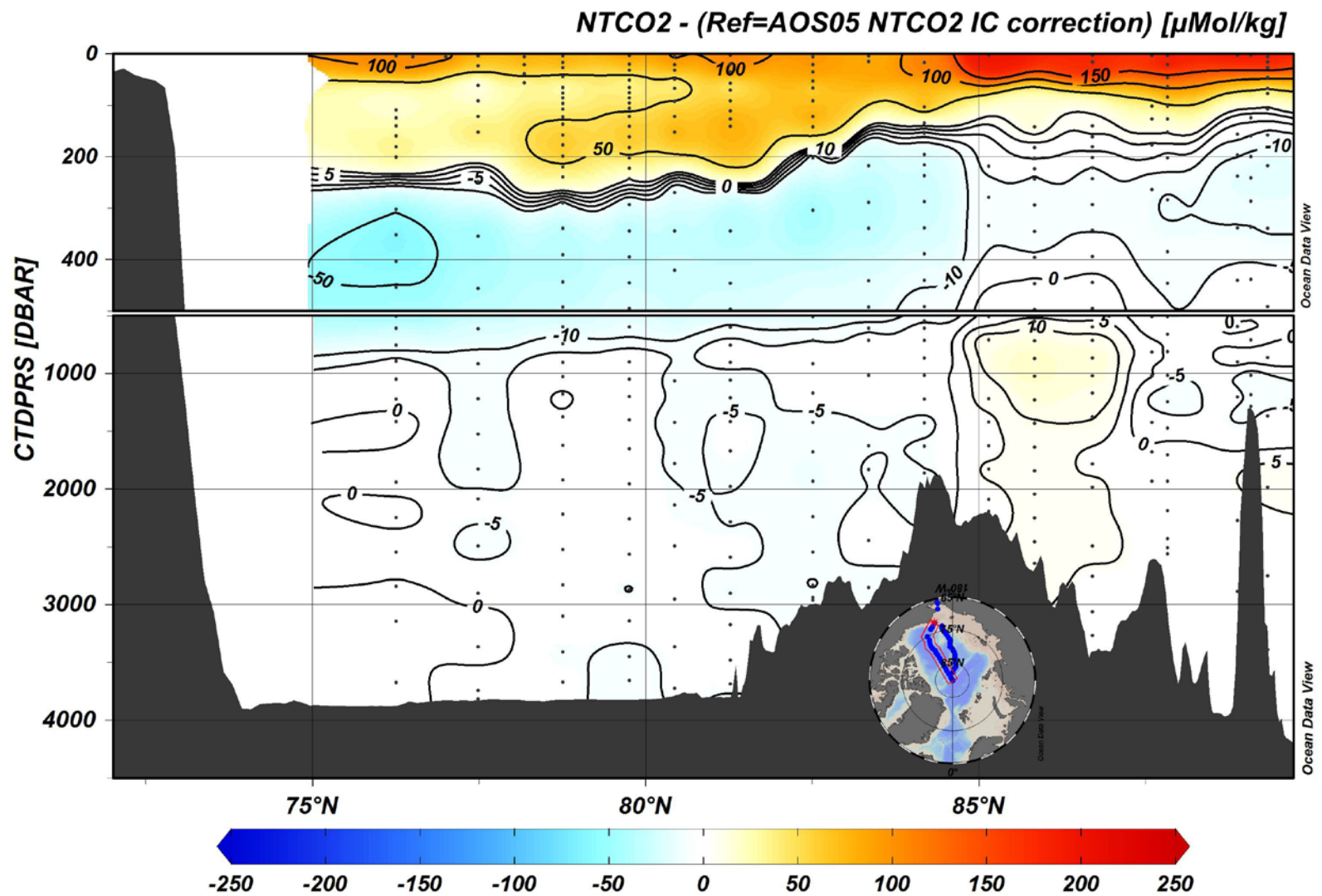


Figure 26. Changes in NTCO₂ between the 2005 and 2015 occupations of the Canada Basin section.

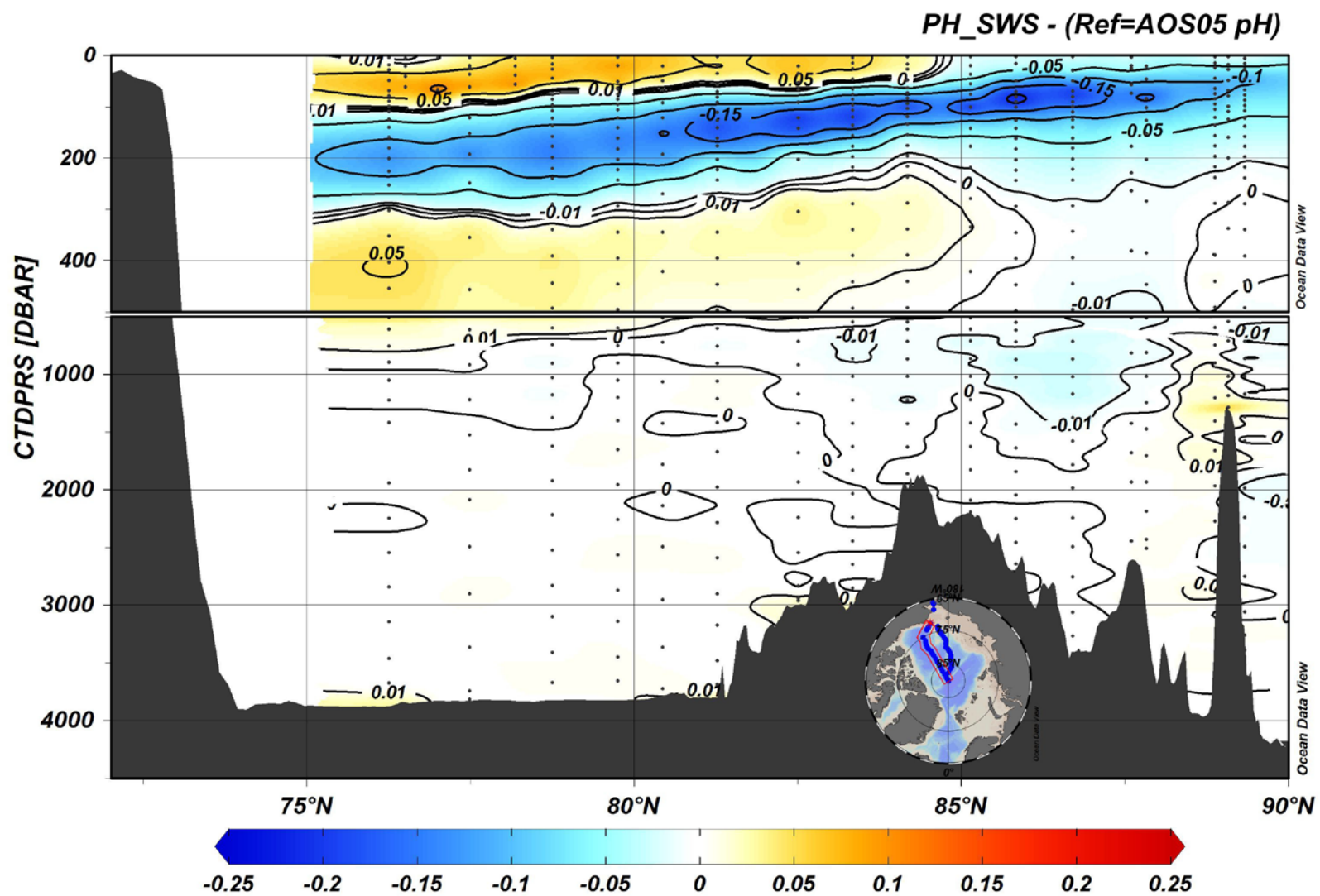


Figure 27. Changes in pH between the 2005 and 2015 occupations of the Canada Basin section.

6.3 Changes Between the AOS94 and the GO-SHIP ARC01

Figure 28 shows that TA remained generally constant in the deep waters between the 1994 and 2015 cruises ($-5.4 \pm 7.7 \mu\text{mol}\cdot\text{kg}^{-1}$). The surface waters showed large decreases of similar magnitude to those found in the Canada Basin. The NTA (figure 29) shows large increases in the surface indicating melting sea ice contains some amount of alkalinity. Changes in TCO_2 and NTCO_2 are shown in figure 30 and 31, respectively. The TCO_2 shows very large decreases in the surface, while the NTCO_2 shows large increases. This is likely a result of ice melt, as was found in section 6.2. The pH was not directly measured on the 1994 cruise and is not shown here.

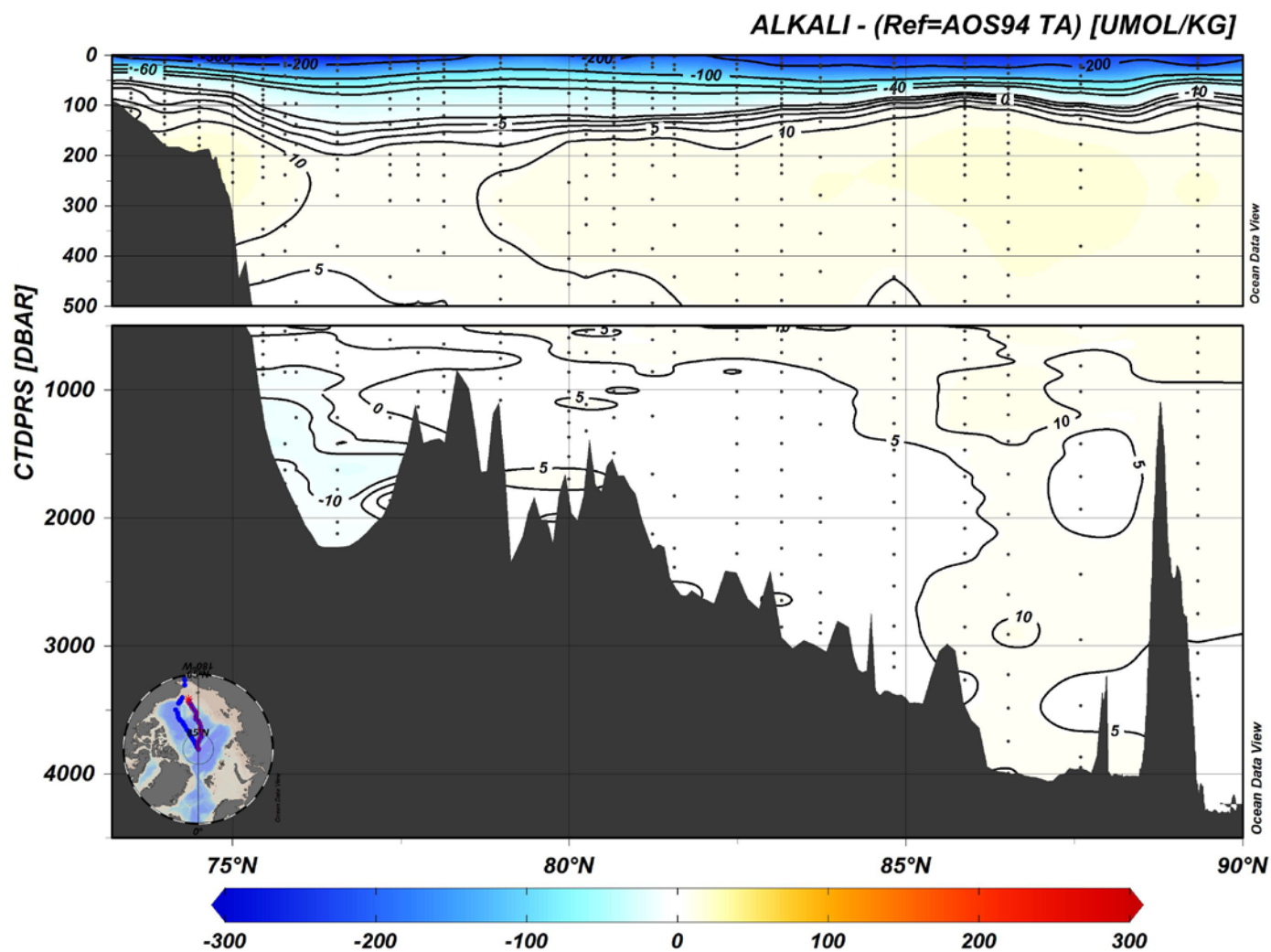


Figure 28. Changes in TA between 1994 and 2015 occupations of Makarov Basin section.

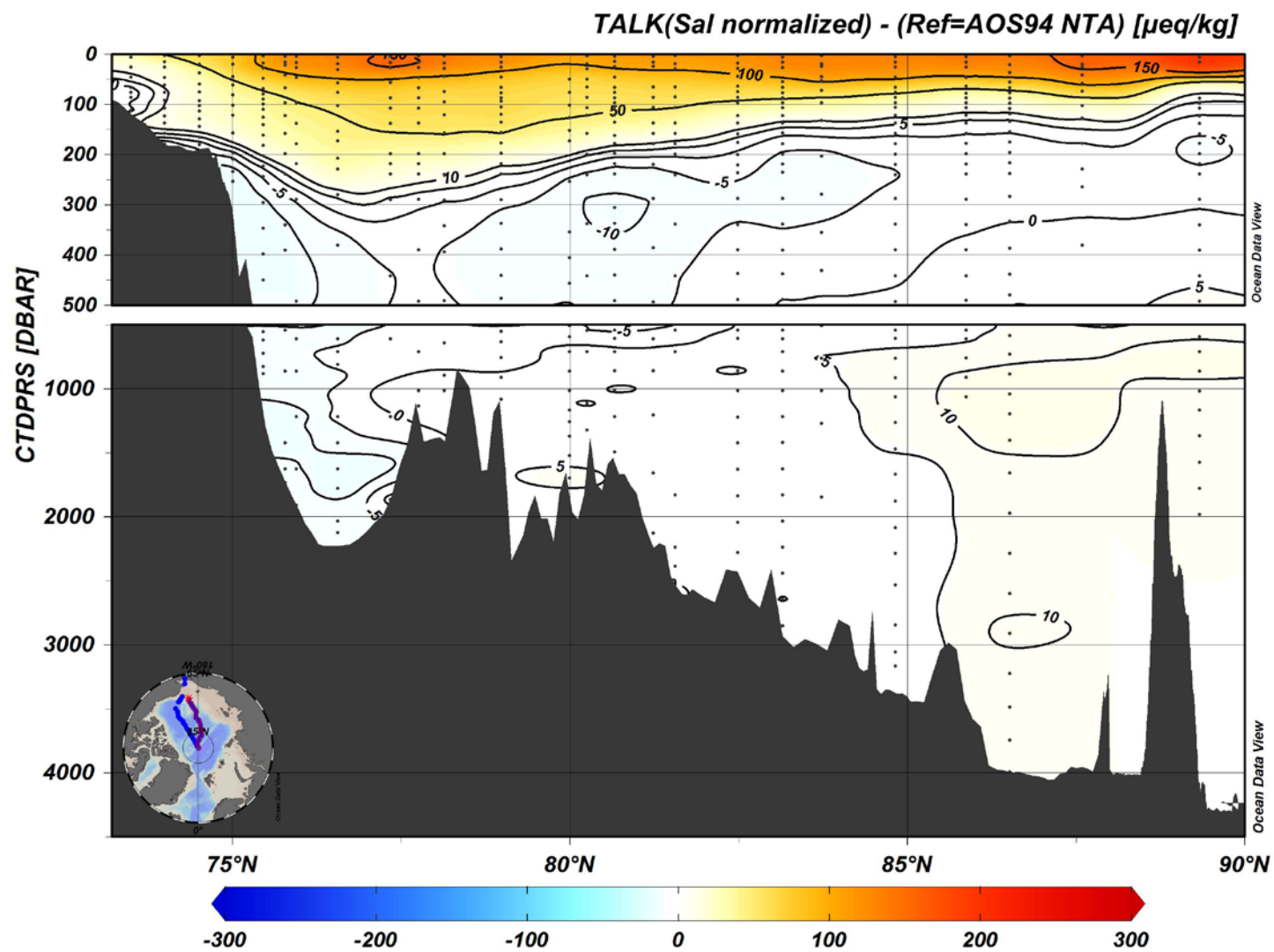


Figure 29. Changes in NTA between 1994 and 2015 in the Makarov Basin section.

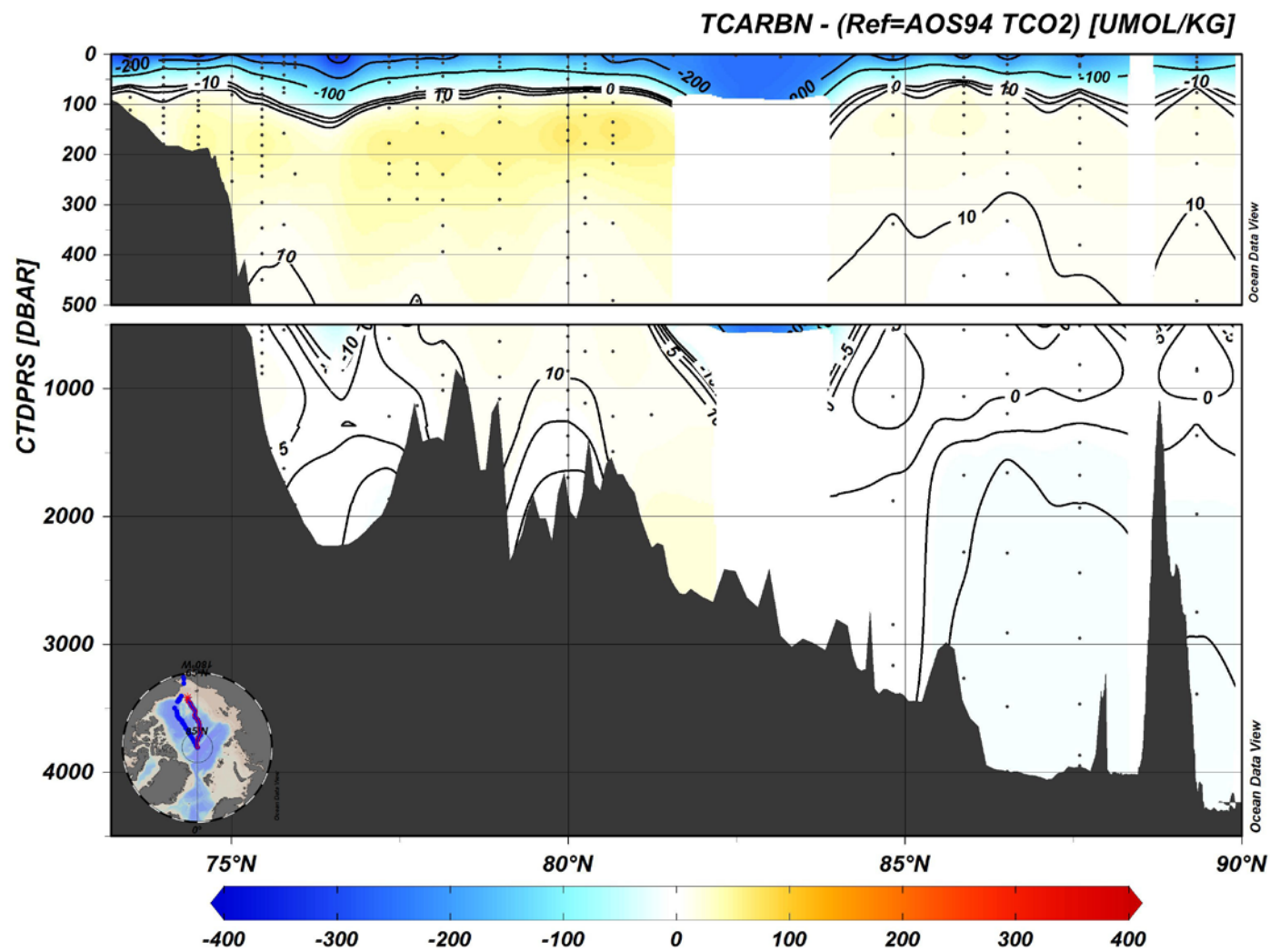


Figure 30. Changes in TCO₂ between 1994 and 2015 occupations of the Makarov Basin section.

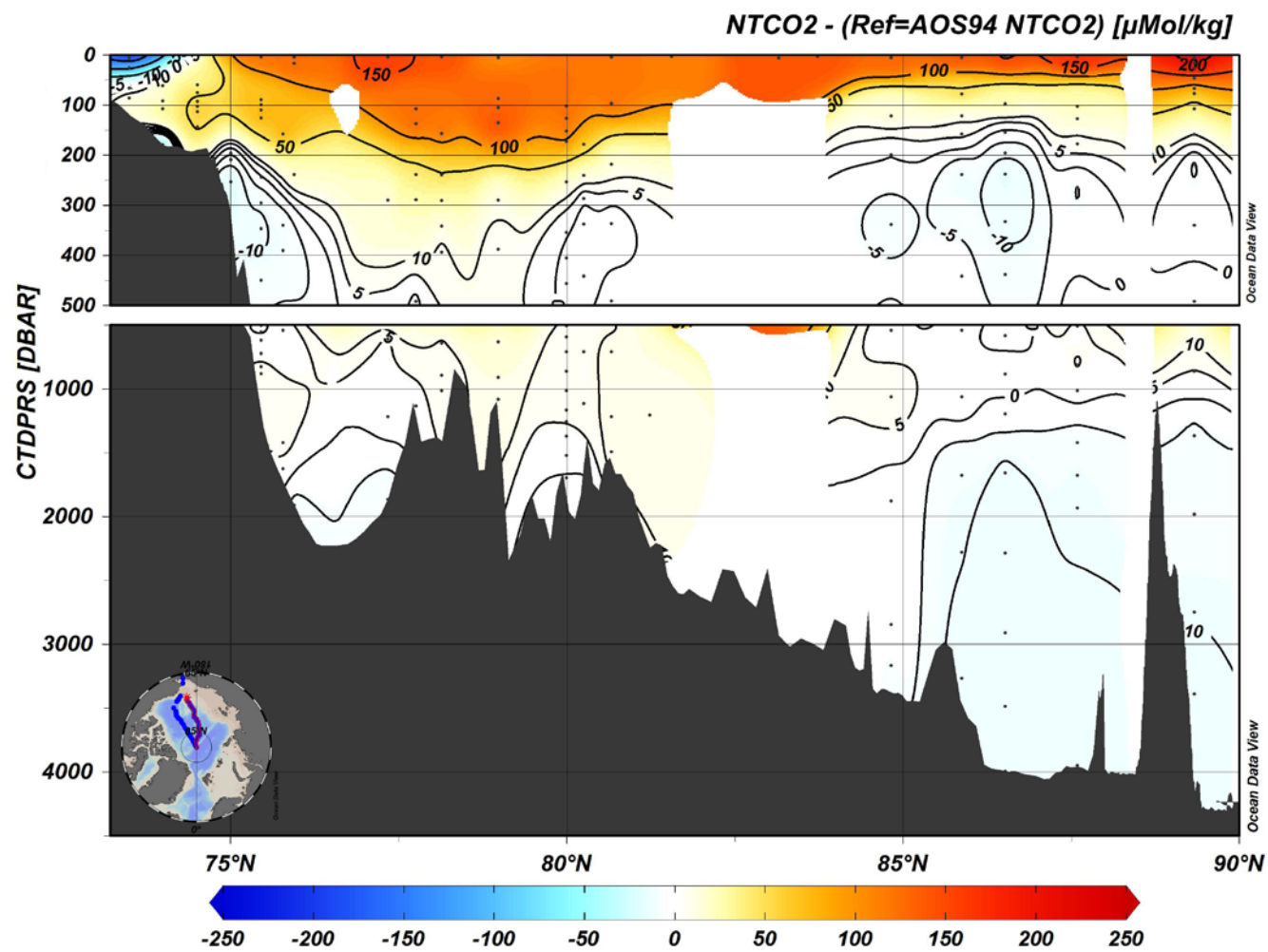


Figure 31. Changes in NTCO₂ between the 1994 and 2015 occupations of the Makarov Basin section.

References

- Clayton, T.D., and R.H. Byrne (1993), Spectrophotometric seawater pH measurements: Total hydrogen ion concentration scale calibration of m-cresol purple and at-sea results. *Deep-Sea Res.*, **40**, 2315-2329.
- Dickson, A.G. (1981), An exact definition of total alkalinity and a procedure for the estimation of alkalinity and total CO₂ from titration data. *Deep-Sea Res., Part A*, **28**, 609-623.
- Dickson, A.G. (1990), Thermodynamics of the dissociation of boric acid in synthetic seawater from 273.15 to 318.15 K. *Deep-Sea Res., Part A*, **37**, 755-766.
- Dickson, A.G., and J.P. Riley (1979), The estimation of acid dissociation constants in seawater media from potentiometric titration with strong base, 1: The ionic product of water-K_{SUS}-w. *Mar. Chem.*, **7**, 89-99.
- Dickson, A.G., C.L. Sabine, and J.R. Christian (Eds.) (2007), [Guide to best practices for ocean CO₂ measurements](#). PICES Special Publication 3, 191 pp.
- Johnson, K.M. (1992). Operator's manual: Single operator multiparameter metabolic analyzer (SOMMA) for total carbon dioxide (CT) with coulometric detection. Brookhaven National Laboratory, Brookhaven, N.Y., 70 pp.
- Johansson, O., and M. Wedborg (1982), On the evaluation of potentiometric titrations of seawater with hydrochloric acid. *Oceanologica Acta*, **5**, 209-218.
- Johnson, K.M., A.E. King, and J.M.N. Sieburth (1985), Coulometric TCO₂ analyses for marine studies: An introduction. *Mar. Chem.*, **16**, 61-82. DOI:10.1016/0304-4203(85)90028-3
- Johnson, K.M., P.J. Williams, L. Brandstrom, and J.M.N. Sieburth (1987), Coulometric total carbon analysis for marine studies: Automation and calibration. *Mar. Chem.*, **21**, 117-133.
- Johnson, K.M., K.D. Wills, D.B. Butler, W.K. Johnson, and C.S. Wong (1993), Coulometric total carbon dioxide analysis for marine studies: Maximizing the performance of an automated continuous gas extraction system and coulometric detector. *Mar. Chem.*, **44**, 167-189.
- Key, R.M., A. Olsen, S. van Heuven, S. K. Lauvset, A. Velo, X. Lin, C. Schirnick, A. Kozyr, T. Tanhua, M. Hoppema, S. Jutterström, R. Steinfeldt, E. Jeansson, M. Ishi, F. F. Perez, and T. Suzuki. (2015), Global Ocean Data Analysis Project, Version 2 (GLODAPv2), ORNL/CDIAC-162, ND-P093. Carbon Dioxide Information Analysis Center, Oak Ridge National Laboratory, US Department of Energy, Oak Ridge, Tennessee. doi: 10.3334/CDIAC/OTG.NDP093_GLODAPv2.

- Lee, K., F.J. Millero and D.M. Campbell (1996), The reliability of the thermodynamic constants for the dissociation carbonic acid in seawater. *Mar. Chem.*, **55** 233-246.
- Lee, K., T-W. Kim, R.H. Byrne, F.J. Millero, R.A. Feely, and Y-M. Liu (2010), The universal ratio of boron to chlorinity for the North Pacific and North Atlantic oceans. *Geochim. Cosmochim. Acta*, **74**, 1801-1811.
- Liu, X., M.C. Patsavas, and R.H. Byrne (2011), Purification and Characterization of meta-Cresol Purple for Spectrophotometric Seawater pH Measurements. *Envir. Sci. and Tech.*, **45**, 4862-4868. DOI:10.1021/es2006665d
- Millero F.J. (2007), The Marine Inorganic Carbon Cycle. *Chem. Rev.*, **107**(2), 308-341.
- Millero F.J., J.-Z. Zhang, S. Fiol, S. Sotolongo, R. Roy, K. Lee, and S. Mane (1993a), The use of buffers to measure the pH of seawater. *Mar. Chem.*, **44**, 143-152.
- Millero, F.J., J.-Z. Zhang, K. Lee, and D.M. Campbell (1993b), Titration alkalinity of seawater. *Mar. Chem.*, **44**, 153-165.
- Millero, F.J., T. Graham, F. Huang, H. Bustos, and D. Pierrot (2006), Dissociation constants for carbonic acid in seawater as a function of temperature and salinity. *Mar. Chem.*, **100**, 80-94.
- Pierrot, D., E. Lewis, D.W.R. Wallace (2006), MS Excel Program Developed for CO₂ System Calculations. ORNL/CDIAC-105a Carbon Dioxide Information Analysis Center, Oak Ridge National Laboratory, U.S. Department of Energy, Oak Ridge, Tennessee. http://dx.doi.org/10.3334/CDIAC/otg.CO2SYS_XLS_CDIAC105a.
- Ramette, R.W., C.H. Culberson, and R.G. Bates (1977), Acid base properties of tris (hydroxymethyl) aminomethane (tris) buffers in seawater from 5 to 40°C. *Analytical Chemistry*, **49**, 867-870.
- Schlitzer, R. (2016), Ocean Data View 4, <http://odv.awi.de>.
- Wilke, R.J., D.W.R. Wallace, and K.M. Johnson (1993) Water-based gravimetric method for the determination of gas loop volume. *Anal. Chem.*, **65**, 2403-2406.

Appendices

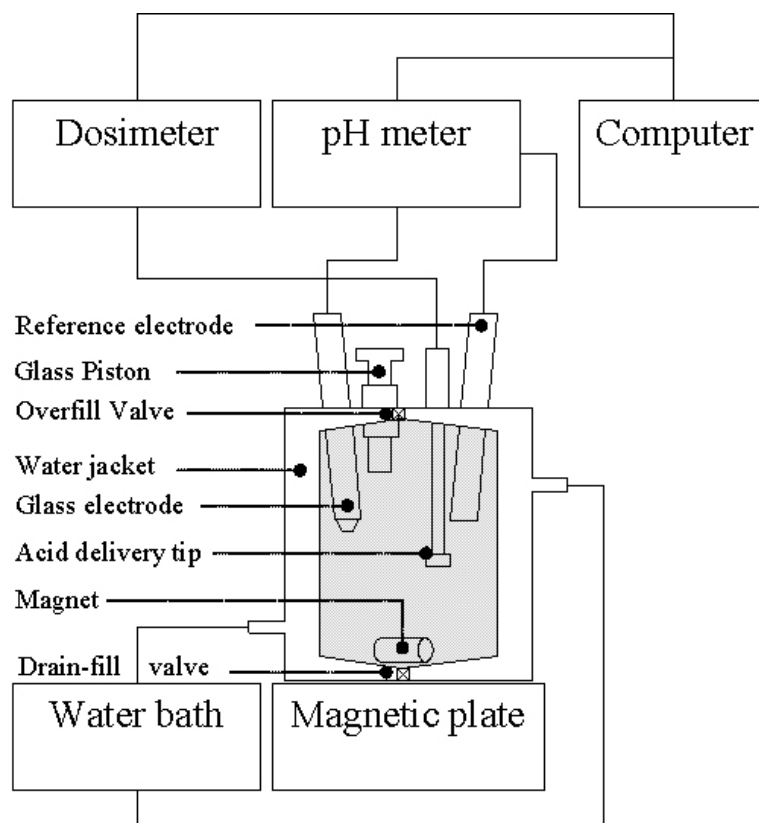
A. Waypoint Coordinates and Bottom Depth of the ARC01 2015 Cruise

Station	Date	Latitude	Longitude	Bottom Depth (m)
1	8/12/2015	60.252	-179.066	750
2	8/14/2015	62.2018	-171.586	49
3	8/15/2015	64.0069	-166.626	33
4	8/16/2015	65.8093	-168.618	54
5	8/16/2015	66.3318	-168.9	58
6	8/16/2015	68.0064	-168.05	57
7	8/18/2015	73.4879	-168.848	118
8	8/18/2015	73.9852	-168.776	191
9	8/19/2015	74.5026	-168.86	198
10	8/19/2015	74.9993	-170.042	260
11	8/20/2015	75.4494	-170.564	358
12	8/20/2015	75.7749	-171.374	1717
13	8/20/2015	75.942	-171.664	1892
14	8/20/2015	76.5108	-173.034	2255
15	8/22/2015	77.3379	-175.062	1846
16	8/22/2015	77.7524	-176.246	1135
17	8/22/2015	78.1354	-176.756	1010
18	8/23/2015	78.977	-175.719	1078
19	8/23/2015	79.9967	-174.962	2099
20	8/25/2015	80.2463	-177.667	2046
21	8/25/2015	80.6578	-179.893	1480
22	8/25/2015	81.2327	179.0976	2227
23	8/26/2015	81.5572	176.8727	2468
24	8/26/2015	82.4804	174.9966	2394
25	8/27/2015	83.1489	173.9356	3021
26	8/27/2015	83.7546	174.915	2938
27	8/29/2015	84.819	170.6886	3335
28	8/30/2015	85.8654	167.044	3740
29	8/31/2015	86.5134	173.464	3932
30	9/1/2015	87.5198	180.1914	3943

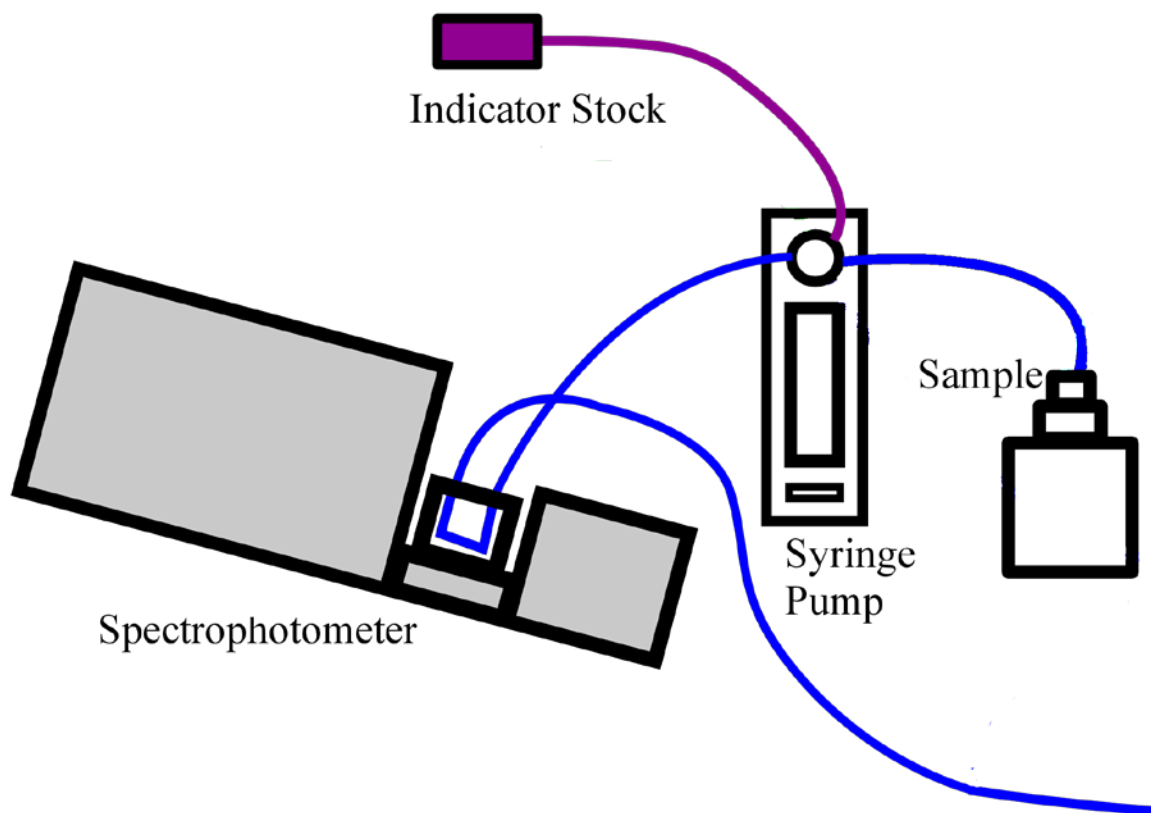
Appendix A Cont.

Station	Date	Latitude	Longitude	Bottom Depth (m)
32	9/5/2015	89.9874	33.0087	4236
34	9/8/2015	89.9466	-96.8591	4221
35	9/8/2015	89.3269	-149.2803	3312
36	9/8/2015	89.0741	-150.4833	1273
37	9/9/2015	88.8741	-149.6064	3857
38	9/10/2015	87.8259	-149.6801	2550
40	9/12/2015	86.6974	-149.2945	3417
41	9/13/2015	85.83	-150.1926	2702
43	9/15/2015	85.135	-150.0627	2204
44	9/17/2015	84.173	-150.0233	2002
45	9/18/2015	83.3372	-150.0632	3084
46	9/19/2015	82.4907	-149.8719	3026
47	9/21/2015	81.2685	-149.9484	3794
48	9/22/2015	80.3694	-149.8547	3859
49	9/25/2015	79.75	-149.5632	3878
50	9/26/2015	78.7493	-147.955	3810
51	9/26/2015	78.1739	-147.8331	3826
52	9/27/2015	77.5027	-148.0085	3829
53	9/28/2015	76.9979	-148.801	3831
54	9/28/2015	76.4954	-149.5013	3834
55	9/29/2015	76.2504	-150.0779	3833
56	9/29/2015	75.0053	-149.8595	3829
57	10/2/2015	73.5056	-156.8083	3465
58	10/4/2015	73.1859	-157.8317	2569
59	10/4/2015	73.0568	-158.5972	1590
60	10/4/2015	72.9989	-158.8455	906
61	10/5/2015	72.7978	-159.6242	125
62	10/6/2015	72.9461	-159.1795	296
63	10/6/2015	72.8487	-159.5407	173
64	10/6/2015	73.0007	-158.9558	523
65	10/6/2015	72.7244	-159.9235	71
66	10/7/2015	71.9966	-162.496	34

B. Diagram of an Automated Total Alkalinity System



C. Diagram of an Automated pH System



D. Data Format Description

FIELD NAME	DESCRIPTION	UNITS
Lat	Latitude	°N
Lon	Longitude	°E
Depth	Depth	m
P	Pressure	db
S	Salinity	S _p
T	Temperature	°C
θ	Potential Temperature	°C
pH _{pot}	Potentiometric pH	
pH _{spec}	Spectrophotometric pH	
TA	Total Alkalinity	μmol·kg ⁻¹
TCO ₂	Total Inorganic Carbon Dioxide	μmol·kg ⁻¹
NTA	Normalized TA to a salinity of 35	μmol·kg ⁻¹
NTCO ₂	Normalized TCO ₂ to a salinity of 35	μmol·kg ⁻¹